NTIA Report 89-250

Power Spectral Densities for Selected Digital Phase-Continuous MFSK Emissions

M. Nesenbergs
D. L. Smith
L. T. Jones

U.S. DEPARTMENT OF COMMERCE
Robert A. Mosbacher, Secretary

Janice Obuchowski, Assistant Secretary
for Communications and Information

October 1989

CONTENTS

FIGURES

FIGURES (cont.)

POWER SPECTRAL DENSITIES FOR SELECTED DIGITAL PHASE-CONTINUOUS MFSK EMISSIONS

M. Nesenbergs, D. L. Smith, and L. T. Jones*

This report is a brief outline and a catalog of 11 power spectral densities for certain M-ary frequency shift keying waveforms. Spectral equations are displayed in graphical form for easy visualization. The spectra pertain to real signals centered on their carrier frequencies.

The selected waveforms are all phase-continuous with no symbol-to-symbol overlap. The number of keying waveforms, M, varies from 2 to 8. The modulation index, k, is typically 2, and only occasionally assumes values of 1 and 4. In all 11 cases considered one encounters discrete line spectra. The relative power contained in the discrete spectrum turns out to be 1/M for regular square waveforms with no dependence between successive symbols and somewhat larger for the other cases considered here. The asymptotic behavior of the continuous spectral component agrees with the theoretical predictions for very large frequency deviations.

Specific waveform shapes include square (or rectangular) pulses, sine-pulses, raised cosine pulses, and squared raised-cosine pulses. The concluding sections of the report cover two special systems of recent practical interest. They are the M=4 and k=2, alternating frequency, format of Rockwell/Collins** and the M=8, k=2, scheme developed by MITRE and Harris Corporations.

Key words: asymptotics; continuous and line spectra; M-ary frequency shift keying (MFSK); phase-continuous waveforms; spectral densities

1. INTRODUCTION AND OVERVIEW

Over the last 30 years, a number of comprehensive studies have addressed the spectral properties of various digital modulations. General properties that apply to large classes of waveforms are known. Also known are special detailed features that pertain to the more unique, practically important, real-world modulation systems. A case that corresponds to both categories is

* The authors are with the Institute for Telecommunicaton Sciences, National Telecommunications and Information Administration, U.S. Department of Commerce, Boulder, CO 80303-3328.

** Certain commmercial equipment and software products are identified in this report to adequately describe the design and conduct of the research or experiment. In no case does such identification imply recommendation or endorsement by the National Telecommunications and Information Administration, nor does it imply that the material or equipment identified is necessarily the best available for the purpose.

that of constant-envelope angle modulation. As the list of references attest, the spectra of the mutually related phase and frequency modulations are well understood, at least on the conceptual level. However, for applications it is often necessary to translate and to condense the theoretical formulas into simpler forms, accompanied by parametric numbers and useful graphs.

This report deals with one subclass of digital frequency modulation (FM). That is the continuous-phase M-ary Frequency Shift Keying (MFSK), for such typical values as M=2, 4, and 8. The frequency deviation or modulation index is in most cases assumed to be k=2, although in a few chosen instances k=1 and 4 are introduced for illustrative purposes. All waveforms are assumed to be non-overlapping in time, that is, from one keying (or symbol, or baud) interval T to the next. For the selected waveform cases, their power spectral densities (or spectral densities, or spectra, for short) are given. When available, published results are used. In other cases, special derivations are made. Formulas are augmented by graphs that emphasize the key features of the MFSK spectra.

The three main characteristics of the continuous-phase MFSK spectra are as follows:

(a) In addition to the continuous spectral density, if certain conditions are met, discrete or line spectra must exist. It will be shown that all waveforms considered here possess spectral lines. With certain exceptions to be noted, the total power in the discrete lines is either equal to or larger than 1/M of the total power. Whether finite or infinite in number, the discrete spectral lines can occur only at certain well-defined frequencies, f. These frequencies correspond to particular, positive and negative, multiples of 1/2T, 1/T, 2/T, etc., or mixtures thereof.

(b) For frequencies that depart from the carrier frequency, f_c, by much, much more than 1/T, the power spectral fall-off depends on the continuity properties of the modulating waveform. The simplest rule of thumb appears to be the following. If the (n-1)-th time derivative of all MFSK pulse sequences is continuous, but the n-th derivative is somewhere discontinuous, then asymptotically the power spectrum must decrease as $1/(f-f_c)^{2(n+2)}$.

(c) The continuous spectra exhibit nearly periodic maxima and minima. For keying interval T, the spacing between minima tends to be either 1/T or 1/2T, while the spacing between peaks is approximately the same as for the minima.

The report is structured as follows. Sections 2 to 6 deal with four-waveform, or M=4, MFSK. The whole development starts with a necessary introduction of notation, plus a summary of the prerequisite theoretical background, in Section 2. (Comment on notation: Since previous writers have chosen widely different symbols to represent the FSK spectra, we include as Appendix A a summary of their power spectrum notation.) Initially, our development is concerned with M=4. However, the context makes it easy to extrapolate to other M values, such as to M=2 in Sections 7 and 8 and to M=8 in Section 10.

Section 3 applies the tools of Section 2 to three square-wave 4FSK waveforms, namely those with index k=1, 2, and 4, respectively. Depending on the data sequence represented, a sequence of these waveforms can have discontinuities at all times that are integer multiples of T.

Section 4 uses the single sine-wave pulse (namely the sinx function between x=0 and $x=\pi$) as the waveform. The index is k=2. The modulating waveform is everywhere continuous, but its first derivative can have discontinuities at times that are integer multiples of T.

Section 5 employs the raised-cosine waveform. It, of course, has a zero slope at multiples of T, and thus a continuous first derivative. The second derivative, however, can have discontinuities.

Section 6 assumes the most complex waveform considered here, namely the square of the raised-cosine waveform. It leads to rather complicated formulas for the spectrum, plus associated computation difficulties. However, since its fourth derivative is the very lowest derivative that can be discontinuous, the associated spectral skirts must fall astoundingly as f to the minus 12-th power.

Section 7 reviews and modifies the spectral expressions for two cases of binary (or M=2) FSK. One is for the deviation index k equal to 1, the other is for k=2.

Section 8 treats the 2FSK with squared raised-cosine waveforms and modulation index k=2. Its asymptotic slope is f^{-12} as it was in Section 6.

Section 9 presents a modified M=4 scheme that exhibits some properties similar to the binary FSK. The unique properties appear to be due to an "alternating frequency-pair" selection rule that is enforced by the modulator. This scheme has been implemented by Rockwell/Collins in some of their systems and, perhaps more noteworthy, it represents a significant proposal for an automated HF system (e.g., link establishment) waveform standard.

Finally, Section 10 shows an 8-ary MFSK. Like many of the earlier cases, its deviation index is k=2, and most of its power spectral properties relate strongly to the corresponding spectra discussed in Section 3 (for M=4) and in Section 7 (for M=2). This 8FSK model represents one more important modem development. At this time, it appears likewise to be a standing candidate for the proposed system standardization effort for automatic link establishment.

Table 1 summarizes the MFSK cases considered in this study. It lists the waveforms, their main spectral features, as well as other key characteristics. It also makes it quite apparent that this report is far from being a comprehensive catalog of all MFSK systems studied here or abroad. Instead, it represents a selective mixture of general interest, the authors' interest, plus a few cases (see Sections 9 and 10) of practical significance in current standardization of radio system designs.

In addition to the previously mentioned Appendix A, which deals with notation, two other appendixes are included here. Their purpose is to remove the mathematical (i.e., trigonometric and Bessel function) details from the main text. The elementary, but often used, trigonometric function properties are collected in Appendix B. Useful Bessel function properties, plus some relevant derivations, are found in Appendix C.

2. COMMON RESULTS FOR 4FSK SYSTEMS

Outline

We seek the power spectral density of a particular class of digital frequency-modulated signals, known as the M-ary FSK or MFSK systems. To have a simpler presentation, assume for time being that M=4. Almost the same general method will later apply to M=2, 8, and other cases.

The present approach is based on the randomness of the modulating data sequence. One estimates the signal auto-correlation function and then uses its Fourier transform to derive the spectral density (Papoulis, 1965). This method has been used by many workers to describe the spectra of certain MFSK

classes (Bennett and Rice, 1963; Anderson and Salz, 1965; Salz, 1965; Prabhu and Rowe, 1974; Rowe and Prabhu, 1975). Whenever possible, previous results are used here without justification or modification. In other instances, modifications and extensions are made as needed.

TABLE 1. Overview of the Phase-Continuous, No Overlap, MSFK Systems Studied in This Report

Pulse Waveform Type	Found In Section	No. FSK Pulses M	Modul. Index k	No. of Discrete Lines	Relative Discrete Power	Asymptotic Peak Envelope
Square Pulse	3	4	1	4	1/4	$(5/8\pi^2)(fT)^{-4}$
" "	3	4	2	4	1/4	$(5/2\pi^2)(fT)^{-4}$
" "	3	4	4	4	1/4	$(10/\pi^2)(fT)^{-4}$
Sine-Pulse	4	4	2	Infinite	.388	$(5/32)(fT)^{-6}$
Raised Cosine	5	4	2	"	.483	$(5/2\pi^2)(fT)^{-8}$
Squared Raised-Cosine	6	4	2	"	.592	$(40/\pi^2)(fT)^{-12}$
Square Pulse	7	2	1	2	1/2	$(1/8\pi^2)(fT)^{-4}$
" "	7	2	2	2	1/2	$(1/2\pi^2)(fT)^{-4}$
Squared Raised-Cosine	8	2	2	Infinite	.748	$(8/\pi^2)(fT)^{-12}$
Rockwell Collins	9	4	2	"	1/2	$(5/2\pi^2)(fT)^{-4}$
MITRE Harris	10	8	2	8	1/8	$(21/2\pi^2)(fT)^{-4}$

To keep matters simple and compatible, the notation of Rowe and Prabhu (1975) is followed in our equations.

The real unity-envelope signal is written as

$$x(t) = \cos(2\pi f_c t + \phi(t)). \tag{1}$$

In (1), f_c is the carrier frequency and $\phi(t)$ is the time-varying phase. The variation of phase is a direct consequence of the MFSK waveforms. When the keying or baud interval has length T, the data source selects a new waveform for every new interval. This selection process is completely memoryless, equiprobable, and random. The waveforms come from a finite alphabet. For M=4 one represents the alphabet as $\{h_1(t), h_2(t), h_3(t), h_4(t)\}$. The phase term is then

$$\phi(t) = \int_{-\infty}^{t} \sum_{n=-\infty}^{\infty} h_{s_n}(\mu - nT)d\mu, \tag{2}$$

where the subscript s_n keeps track of which of the four waveforms is picked in time-slot n by selecting values from the set {1, 2, 3, 4}.

As is commonly done, the actual angle modulation is written as a complex random function

$$v(t) = e^{j\phi(t)}. \tag{3}$$

Its power spectrum, $P_v(f)$, determines the desired double-sideband power spectrum, $P_x(f)$, of the real band limited signal x(t) (Prabhu and Rowe, 1974):

$$P_x(f) = 1/4(P_v(f-f_c) + P_v(-f-f_c)). \tag{4}$$

Or, when the spectrum is divided into its continuous and discrete line components as functions of positive (only) frequencies,

$$P_x(f_c+f)/T = 1/2(P_{xc}(fT) + P_{x1}(fT)). \tag{5}$$

Useful formulas and graphs for (5) represent the ultimate goal of this report. Of course, different system assumptions and parameter values will alter the expressions and shapes for the spectra. Sections 3 to 10 illustrate that point for the selected modulation cases of interest.

Derivation of Spectrum

Start with a finite waveform alphabet, as illustrated in Figure 1 for a single time interval $0 \leq t \leq T$. A number of pertinent properties are noted:

(A) The number of distinct waveforms is M=4.

(B) Frequency modulation with bounded waveforms results in everywhere continuous-phase, as long as spurious phase jumps are not allowed at transition times t=nT.

(C) There is no waveform overlap from one keying interval to the next.

(D) All four waveforms are multiples of a common real, but otherwise arbitrary, generator (or parent) waveform h(t).

(E) The modulation index for the above alphabet is defined as twice the maximum instantaneous phase deviation of the generator waveform h(t):

$$k = 2 \int_0^T h(t)dt. \qquad (6)$$

This definition differs from the term "frequency deviation," which nominally should refer to the largest $|h(t)|$ value in the $0 \leq t \leq T$ interval. To avoid a potential confusion of terms, the mod-index k convention of (6) is adopted here (Taub and Schilling, 1971). Small integer values, such as k=1, 2, 3, ..., are of most practical interest. Most of the examples considered here will have k=2.

To proceed, define a column vector with arbitrary components $\{x_1, x_2, x_3, x_4\}$ as

$$x] = \begin{bmatrix} x_1 \\ x_2 \\ x_3 \\ x_4 \end{bmatrix}. \qquad (7)$$

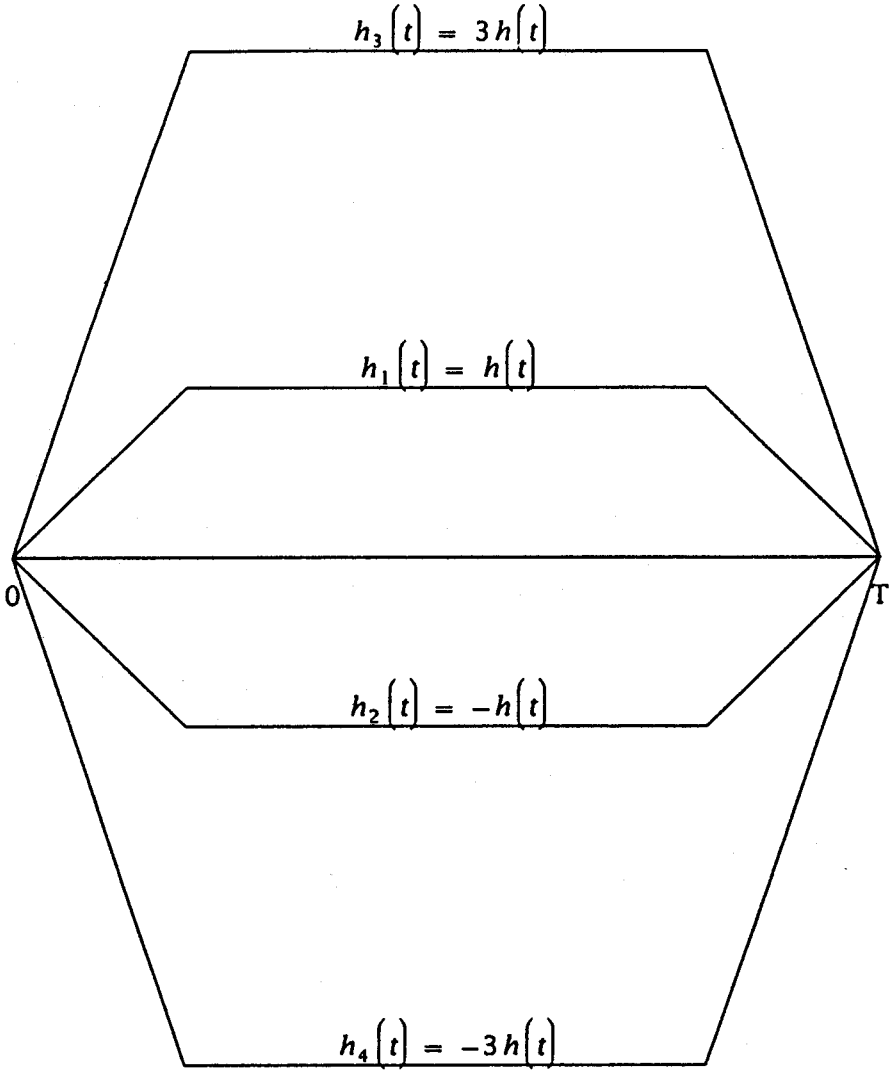

Figure 1. An illustration of an M = 4 waveform alphabet with a single parent h(t).

The transpose of x], or $x]^t = \underline{x}$, is then a row vector. It will occur occasionally in the text. Far more common will be the occurrences of functions of vectors. For any function f(x) and any vector x], we use the natural vector-function convention,

$$f(x]) = \begin{bmatrix} f(x_1) \\ f(x_2) \\ f(x_3) \\ f(x_4) \end{bmatrix}. \tag{8}$$

Based on the above vector notation, the waveform alphabet can be said to be a vector function over $0 \leq t \leq T$,

$$h(t)] = \Delta] \bullet h(t), \tag{9}$$

where the increment or coefficient vector $\Delta]$ is in transpose form

$$\Delta]^t = (1, -1, 3, -3). \tag{10}$$

One next needs to define what can be called a segment of the MFSK baseband,

$$\begin{aligned} q(t)] &= e^{j2\pi\Delta]} \bullet \int_0^t h(\mu)d\mu \qquad \text{for } 0 \leq t \leq T, \\ &= 0] \qquad\qquad\qquad\qquad \text{elsewhere.} \end{aligned} \tag{11}$$

It is followed by the probability weight vector that corresponds to the waveform vector h(t)] in (9),

$$w] = (1/4)1]. \tag{12}$$

where the vector 1] consists entirely of unity components.

Given (6), (11), and (12), one is in a position to carry out the test for the existence of the line spectrum. That test, known to be both necessary and sufficient, states that discrete line spectrum exists when the scalar vector-product, $\underline{w} \cdot q(T)]$, has a magnitude of unity (Rowe and Prabhu, 1975).

For the MFSK model postulated above and for k an integer,

$$\underline{w} \bullet q(T)] = (1/4)(e^{jk\pi} + e^{-jk\pi} + e^{3jk\pi} + e^{-3jk\pi}) = e^{jk\pi}. \qquad (13)$$

Therefore, for all integer values of the modulation index k, the above MFSK model must possess discrete spectral lines.

Further derivation of the continuous and the line spectra can benefit from a Fourier series expansion of q(t)], see (11). A minor problem arises occasionally, when the natural period of q(t)] may not be T, but some $\tau \geq T$. One expands

$$q(t)] = \sum_{n=-\infty}^{\infty} c_n] \bullet e^{j2\pi nt/\tau}, \qquad (14)$$

and notes that quite generally the coefficient vector must be

$$c_n] = (1/\tau) \int_0^{\tau} \hat{q}(t)] \bullet e^{-j2\pi nt/\tau}\, dt, \qquad (15)$$

where $\hat{q}(t)]$ is an extension of q(t)] from $0 \leq t \leq T$ to $0 \leq t \leq \tau$. Thus,

$$\begin{aligned} \hat{q}(t)] &= q(t)] && \text{for } 0 \leq t \leq T, \\ &= \text{"does not matter"} && \text{elsewhere.} \end{aligned} \qquad (16)$$

With the help of the Fourier coefficients, $c_n]$, the Fourier integral transform R(f)] of the MFSK pulses can be written down by inspection.

$$R\ (f)] = \int_0^T q(t)] \bullet e^{-j2\pi ft}\ dt \tag{17}$$

$$= (\tau/j2\pi) \sum_{n=-\infty}^{\infty} c_n] \bullet (1-e^{-2j\pi(fT-nT/\tau)})/(f\tau-n).$$

Equation (17) is the basic form for arbitrary $\tau \geq T$. For specific τ values, R(f)] can be simplified. For instance, $\tau=T$ yields

$$R(f)] = (T/j2\pi)(1-e^{-j2\pi fT}) \sum_{n=-\infty}^{\infty} c_n]/(fT-n)\ , \tag{18}$$

and so on for $\tau=2T$, 3T, etc.

One is finally at a point where the formulas for the complete spectra can be written down. That is true, because both the continuous and the discrete spectra of the angle modulated baseband, see v(t) in (3), are determined by R(f)] as follows.

For the continuous spectral component of the assumed 4MFSK model one has

$$P_{vc}(f) = (\underline{R(f)} \bullet [M] \bullet \overset{*}{R}(f)])/T,$$

$$= \frac{1}{16T} \sum_{1 \leq i \leq j \leq 4} |R_i(f) - R_j(f)|^2, \tag{19}$$

where * denotes the complex conjugate, where [M] is our own shorthand for the Prabhu and Rowe (1974) matrix

$$[M] = (1/4)[I] - (w] \cdot \underline{w})$$

$$= (1/16) \begin{bmatrix} 3 & -1 & -1 & -1 \\ -1 & 3 & -1 & -1 \\ -1 & -1 & 3 & -1 \\ -1 & -1 & -1 & 3 \end{bmatrix}, \tag{20}$$

while $R_i(f)$ and $R_j(f)$ are components of R(f)] in (18) and [I] is the identity matrix.

The corresponding discrete spectrum is given by

$$P_{v1}(f) = (1/\tau^2)|\underline{w} \bullet R(f)]|^2 \bullet \sum_{n=-\infty}^{\infty} \delta(f-n/\tau). \qquad (21)$$

where $\delta(f-n/\tau)$ represents the standard delta or impulse function (Papoulis, 1962) that, subject to non-zero coefficient, can contribute only to a unique discrete frequency, i.e., the n-th multiple of $1/\tau$. When $\tau=T$, spectral lines can occur only at integer values of fT. However, when $\tau=2T$ holds, lines are possible at all n/2. For odd n this allows discrete lines at $fT=\pm 1/2, \pm 3/2, \ldots$, subject to non-vanishing coefficients in (21).

Substitutions of (19) and (21) into (4) and (5) yield the complete spectra of the 4FSK modulations assumed above. Specific cases are illustrated in the Sections to follow.

3. SPECTRA FOR 4FSK WITH SQUARE WAVEFORMS

The summary results of Section 2 are applied here to square or rectangular waveforms. The generating waveform,

$$h(t) = k/2T \qquad \text{for all } 0 \leq t \leq T, \qquad (22)$$

satisfies the modulation index convention of (6). Per (11), one obtains for $0 \leq t \leq T$,

$$q(t)] = e^{j\pi k\Delta] \bullet t/T}. \qquad (23)$$

Its Fourier series expansion is carried out next, followed by all the other terms called for in Section 2. In particular, that includes meticulous evaluations of (15), (17), (19), and (21), plus subsequent substitution into (4) and (5). The end result is the total, continuous plus line, power spectrum.

The expressions turn out different for different values of mod-index k. The diversity starts already in the Fourier series of (14), where the most convenient period τ appears to be T for even k, and 2T for odd k. We treat the distinct k cases separately.

Case for k=1

Set $\tau=2T$ and expand $q(t)]$ into Fourier series (14). The coefficient vector $c_n]$ follows from (15) and (16),

$$c_n] = d(n,\Delta]), \tag{24}$$

where the latter symbol represents a vector or ordered 4-tuple of Kronecker deltas. For any two integers, n and m, the Kronecker delta has the usual meaning,

$$\begin{aligned} d(n,m) &= 1 \qquad \text{if } n=m, \\ &= 0 \qquad \text{otherwise.} \end{aligned} \tag{25}$$

Equation (24) reduces the infinite sum in $R(f)]$ (see (17)) to a single four-component vector,

$$R(f)] = (T/j\pi)(1+e^{-2j\pi fT})/(2fT-\Delta]), \tag{26}$$

which can be readily inserted into the baseband spectra formulas of (19) and (21).

The complete power spectral density, as defined in (5), is

$$\frac{P_x(f_c+f)}{T} = \frac{\cos^2(\pi fT)}{16\pi^2}\left[\frac{1}{(f^2T^2-1/4)^2} + \frac{9}{(f^2T^2-9/4)^2} + \frac{8f^2T^2}{(f^2T^2-1/4)^2(f^2T^2-9/4)^2}\right]$$

$$+ (1/32)\left[\delta(fT-1/2) + \delta(fT+1/2) + \delta(fT-3/2) + \delta(fT+3/2)\right]. \tag{27}$$

The upper half of (27) is the continuous spectrum. The lower half is the four-line discrete spectrum. The complete expression can be inferred from Anderson and Salz (1965).

Both k=1 4FSK spectra are plotted in Figure 2. The display is linear in fT and it covers the main power region around the carrier frequency. Note that the continuous spectrum has three symmetrical peaks, with the outlayers slightly farther than f=1/T from the central peak. The nulls occur at all positive and negative values of fT=5/2, 7/2, 9/2, ... Thus the spacing between adjacent nulls in Figure 2 is 5fT in the center and fT on both sides.

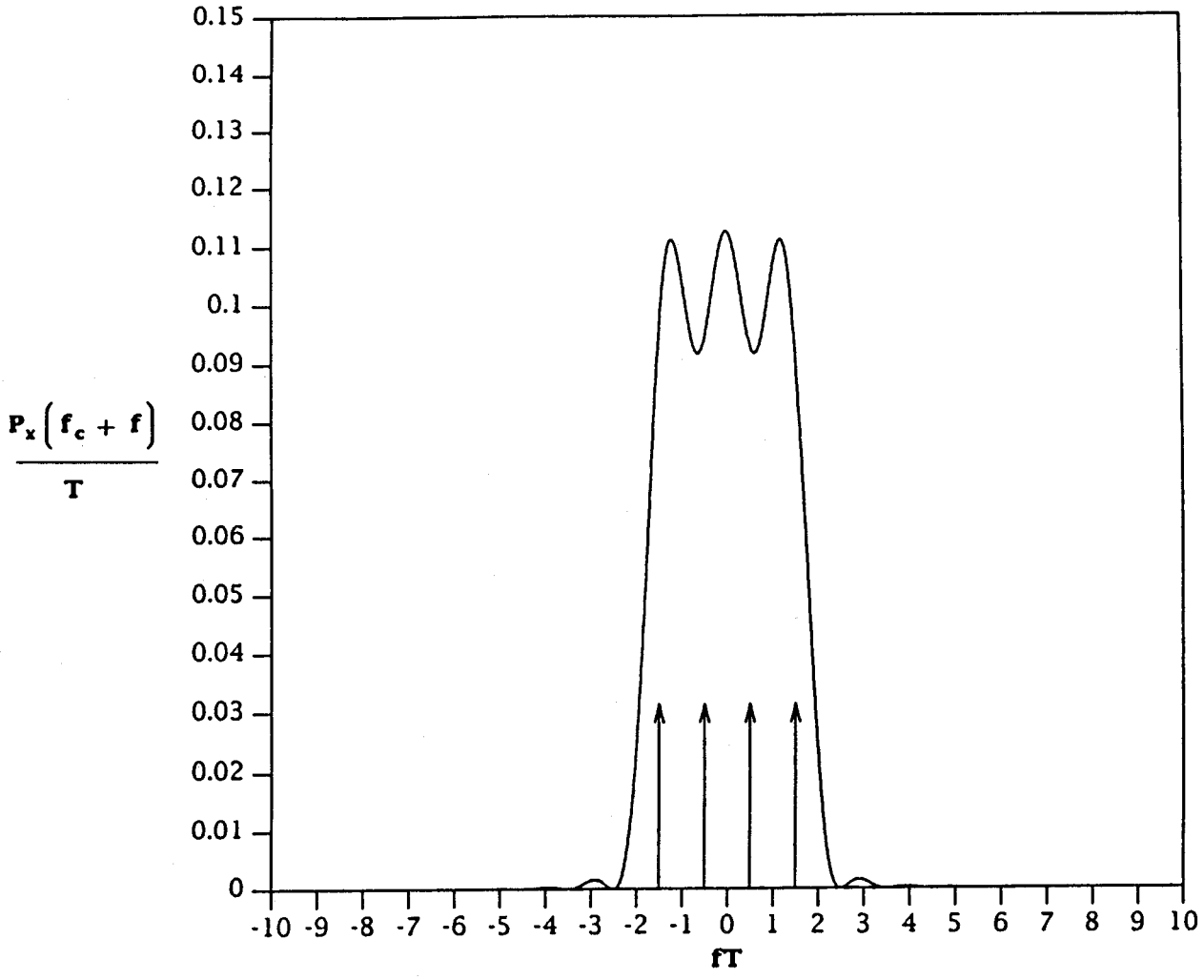

Figure 2. The continuous and discrete spectra of square-wave 4FSK for modulation index k = 1.

The spectral lines are also separated by fT. The listed trigonometric integrals of Appendix B establish that the total continuous power is 3/8. The individual power in a discrete line is 1/32. This verifies that the total power in the frequency modulated signal (1) is 1/2, the total discrete line power is 25 percent thereof, and the remaining 75 percent belongs to the continuous spectrum.

The following comment pertains to this and other MFSK cases. The statements about locations of nulls and percentages of power in various spectral peaks can often be supported theoretically by looking at the equations, such as those in the first half of (27).

The cosine and sine functions cause periodic nulls, unless they are cancelled out by the term in the denominator. To make the null versus no-null recognition easier, the first part of Appendix B contains a number of useful limiting properties for the more common trigonometric functions.

The percentage power in the continuous spectrum can be obtained by direct integration of the appropriate terms in $P_x(f_c + f)/T$. The second part of Appendix B contains a short listing of definite integrals that may expedite this process in many practical instances.

Figure 3 plots the k=1 continuous spectrum on a logarithmic fT scale. This type of graph is an expedient way to illustrate the asymptotic behavior of the spectrum for large values of fT. Note that for very large fT the peak spectral envelope falls off as $(5/8\pi^2)(fT)^{-4}$, which is expected for FSK with discontinuous keying waveforms (see characteristic (b) in the Introduction).

Case for k=2

Set τ=T and observe that the same Fourier coefficients of (24) apply to the Fourier series for k=1 and k=2. It follows from (18) that

$$R(f)] = (T/j2\pi)(1-e^{-j2\pi fT})/(fT-\Delta]). \qquad (28)$$

The complete power spectrum for rectangular, k=2, 4FSK is then:

$$\frac{P_x(f_c+f)}{T} = \frac{\sin^2(\pi fT)}{4\pi^2}\left[\frac{1}{(f^2T^2-1)^2} + \frac{9}{(f^2T^2-9)^2} + \frac{32f^2T^2}{(f^2T^2-1)^2(f^2T^2-9)^2}\right] \qquad (29)$$
$$+ (1/32)\left[\delta(fT-1) + \delta(fT+1) + \delta(fT-3) + \delta(fT+3)\right].$$

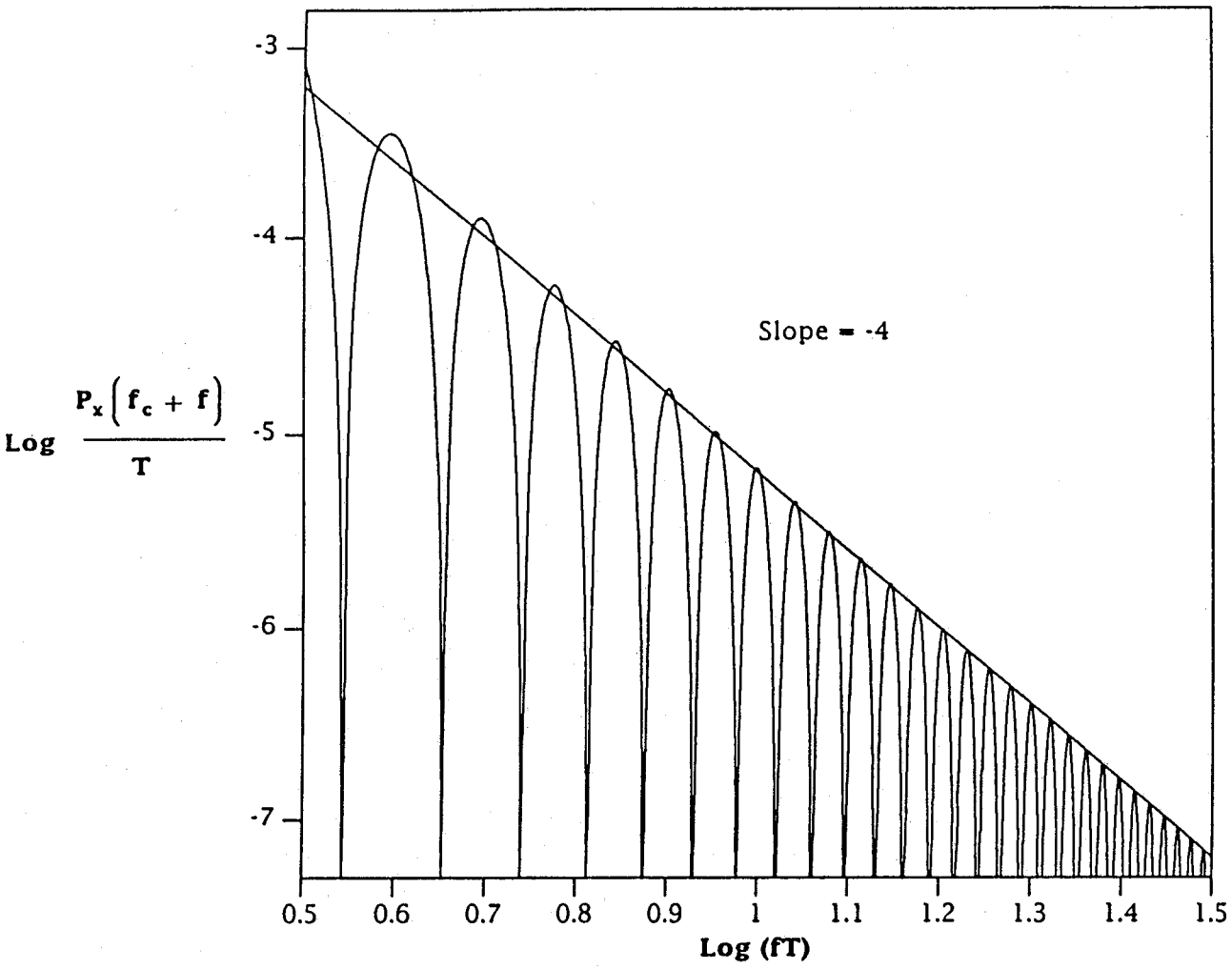

Figure 3. The asymptotic continuous spectral behavior of the k = 1, square-wave, 4FSK for large frequencies.

As before, the first half of this is the continuous spectrum and the second half is the discrete line spectrum. For comparison, similar spectra are found in Anderson and Salz (1965).

Both the continuous and the discrete components of (29) are shown in Figure 4. The horizontal and vertical scales are linear. The main bulk of the continuous power is concentrated in four spectral peaks that center near fT=-3, -1, 1, and 3. In the central region nulls are separated by two fT units, but further out that separation becomes one fT unit.

The four discrete lines are roughly collocated with the continuous maxima. Appendix B again proves that the continuous spectrum integrates to 3/8. The total discrete line power is still 25 percent, as it was in the k=1 case considered earlier.

Figure 5 presents the log-log plot for large fT. The asymptotic peak envelope falls off as $(5/2\pi^2)(fT)^{-4}$, as is determined from (29).

Case for k=4

Set τ=T and note that the Fourier coefficients are now given by

$$c_n] = d(n,2\Delta]), \tag{30}$$

where the Kronecker delta is defined as in (25). But then,

$$R(f)] = (T/j2\pi)(1-e^{-j2\pi fT})/(fT-2\Delta]), \tag{31}$$

and the complete power spectral density of the rectangular, k=4, 4FSK is

$$\frac{P_x(f_c+f)}{T} = \frac{\sin^2(\pi fT)}{\pi^2}\left[\frac{1}{(f^2T^2-4)^2} + \frac{9}{(f^2T^2-36)^2} + \frac{128f^2T^2}{(f^2T^2-4)^2(f^2T^2-36)^2}\right] + \left[(1/32)\quad \delta(fT-2) + \delta(fT+2) + \delta(fT-6) + \delta(fT+6)\right]. \tag{32}$$

The two halves of this spectrum, namely the continuous and the discrete components, behave in a manner consistent with previous derivations.

The central part of the power spectrum (32) is displayed in Figure 6. The coordinate axes are linear as in Figures 2 and 4. Note that the power of

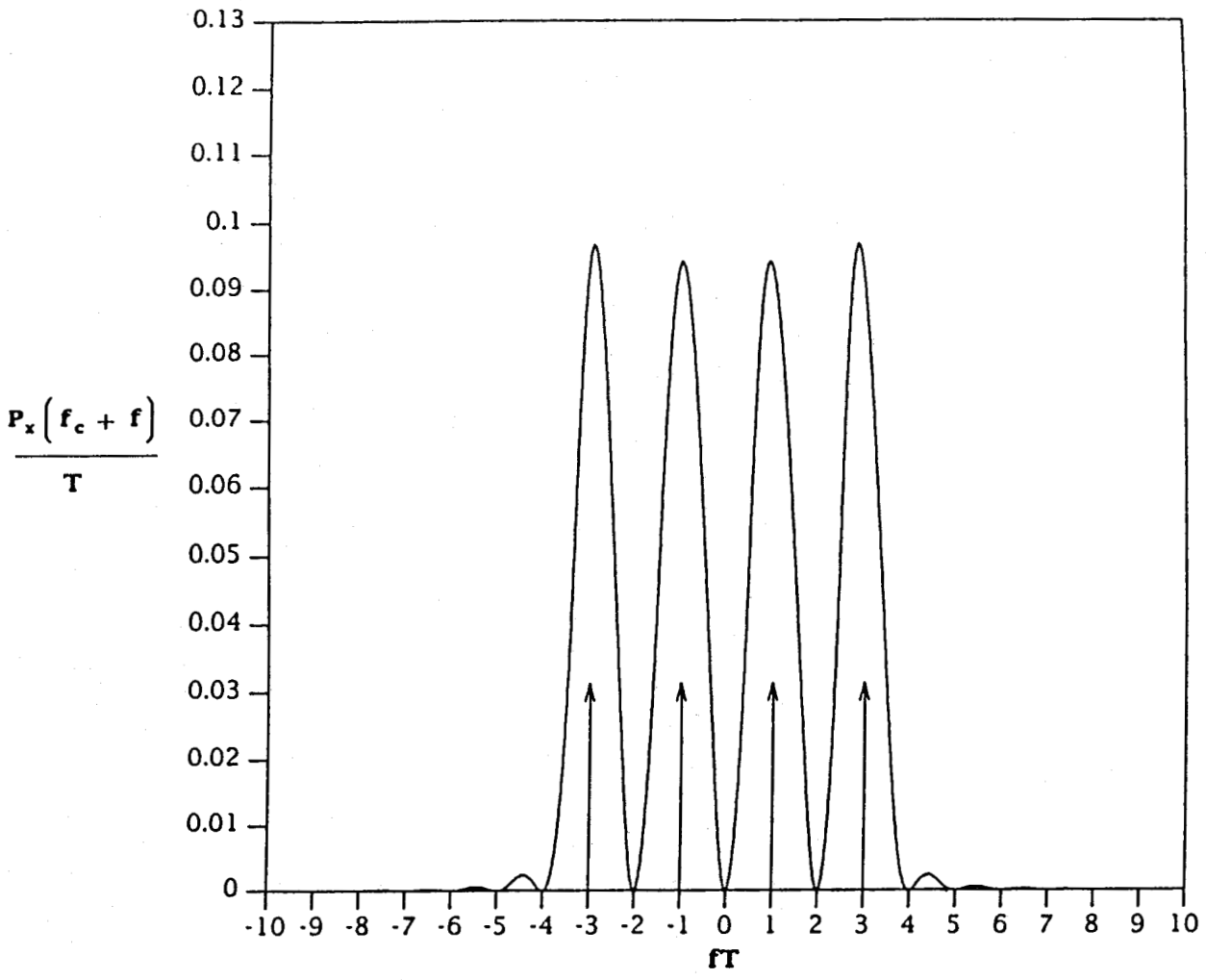

Figure 4. The continuous and discrete spectra of square-wave 4FSK for modulation index k = 2.

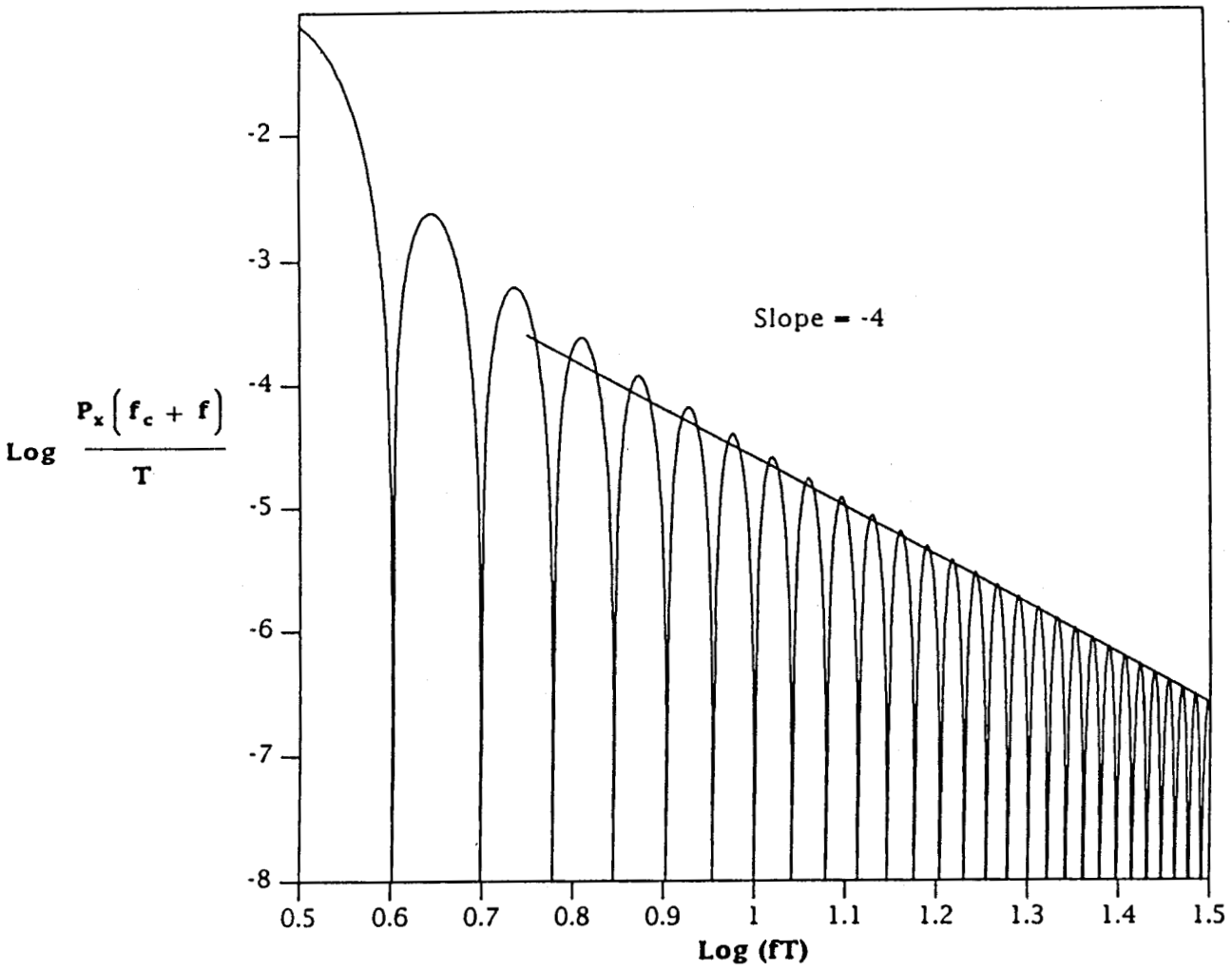

Figure 5. The asymptotic continuous spectral behavior of the k = 2, square-wave, 4FSK for large frequencies.

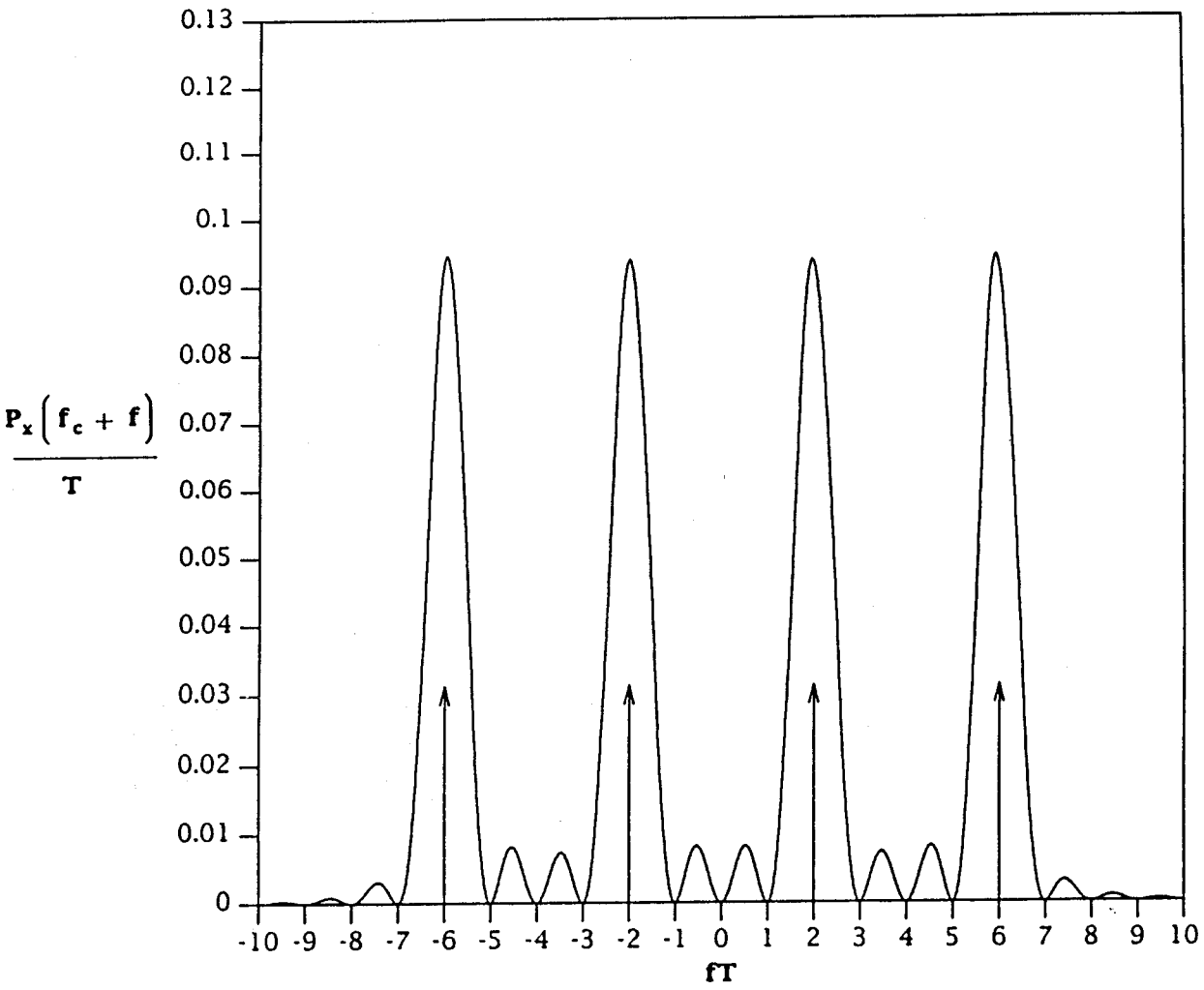

Figure 6. The continuous and discrete spectra of square-wave 4FSK for modulation index k = 4.

the continuous component is centered around fT=-6, -2, 2, 6, which as before coincides with the locations of the four discrete spectral lines. Thus, the main peaks, including the delta functions, are separated by four fT units. The nulls are nominally one unit apart, except at the main peaks, where the separation is double. As in the previous cases of this Section, exactly 25 percent of the total power belongs to the discrete spectrum.

Figure 7 illustrates the asymptotic behavior of the k=4 case. Because of the logarithmic scales, the "minus four" slope of the analytically derived $(10/\pi^2)(fT)^{-4}$ is quite apparent.

4. SPECTRA FOR 4FSK WITH SINE-PULSE WAVEFORMS

Consider the generator waveform to be a half-period upward loop of a sinewave. One calls,

$$h(t) = (\pi k/4T)\sin(\pi t/T) \qquad \text{for } 0 \leq t \leq T, \tag{33}$$

the sine pulse with modulation index k. For convenience, let k be an even integer. Then

$$q(t)] = e^{j\pi(k/2)\Delta]}\ (1-\cos(\pi t/T)) \tag{34}$$

remains to be expanded in Fourier series (14). To benefit from the full-cycle symmetry of the sinewave, set $\tau=2T$. Then apply one particular version of the Bessel generating function (see Appendix C or Watson, 1962),

$$e^{jz\cos\theta} = \sum_{n=-\infty}^{\infty} j^n J_n(z) e^{jn\theta}, \tag{35}$$

to (34) with integer valued k/2. The result is an identity for Fourier coefficients,

$$c_n] = (1/j^n)e^{j\pi(k/2)\Delta]}J_n(\pi(k/2)\Delta]). \tag{36}$$

Substitution into (17) yields

$$R(f)] = Te^{-j\pi(fT-(k/2)\Delta])} \sum_{n=-\infty}^{\infty} J_n(\pi(k/2)\Delta])\ \frac{\sin\pi(fT-n/2)}{\pi(fT-n/2)}\ . \tag{37}$$

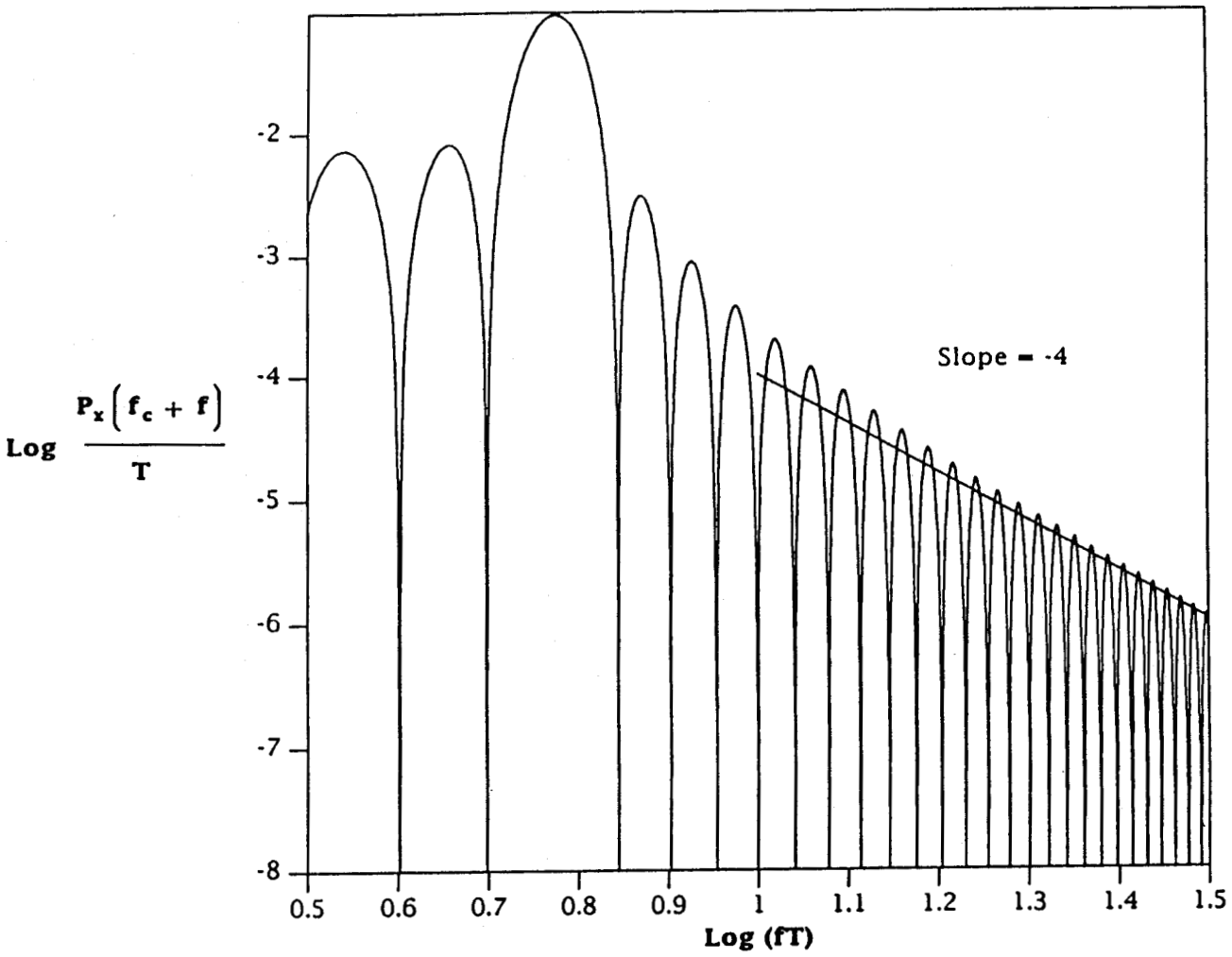

Figure 7. The asymptotic continuous spectral behavior of the k = 4, square-wave, 4FSK for large frequencies.

The ultimate expressions for the power spectrum are simpler if one introduces for $\nu=1, 3$ the following two entities:

$$A_\nu(fT) = \frac{J_0(\nu k\pi/2)}{fT} + 2fT \sum_{m=1}^{\infty} (-1)^m \frac{J_{2m}(\nu k\pi/2)}{f^2T^2-m^2}, \qquad (38)$$

$$B_\nu(fT) = 2fT \sum_{m=0}^{\infty} (-1)^m \frac{J_{2m+1}(\nu k\pi/2)}{f^2T^2-(m+(1/2))^2}.$$

The power spectrum for the 4FSK, with sine pulse waveforms and modulation index k an even integer, is then

$$\frac{P_x(f_c+f)}{T} = \frac{1}{8\pi^2}\left[(A_1(fT) - A_3(fT))^2\sin^2(\pi fT) + 2(B_1^2(fT) + B_3^2(fT))\cos^2(\pi fT)\right] + (1/8)\sum_{n=-\infty}^{\infty} (J_{2n}(k\pi/2) + J_{2n}(3k\pi/2))^2\delta(fT-n). \qquad (39)$$

As before, the upper half of the spectrum is the continuous part. The lower half is the discrete line spectrum.

Figure 8 shows the total, continuous plus discrete, spectrum of (39) for the special case k=2. The graph emphasizes the center of the band, which coincides with the symmetric region around f=0. The coordinate axes are both linear. There are four main peaks located approximately at fT values of ±1.3 and ±3.9. The central peaks are the largest. At f=0, (39) indicates that the spectrum does not have a null, but a value of $(J_0(\pi)-J_0(3\pi))^2/8=.002$. Nulls do, however, occur near fT=±2.8 and at other higher frequency deviations from the carrier.

The discrete spectrum has infinitely many lines. The lines are located at frequencies that are integer multiples of 1/T. The lengths of the arrows represent the amplitudes of the delta functions. Their numerical values agree with the ordinate axis in the figure. The total discrete line power, as shown in Appendix C, is

$$(1/8)\sum_{n=-\infty}^{\infty} (J_{2n}(k\pi/2)+J_{2n}(3k\pi/2))^2 = (1/16)(2+3J_0(k\pi)+2J_0(2k\pi)+J_0(3k\pi)). \qquad (40)$$

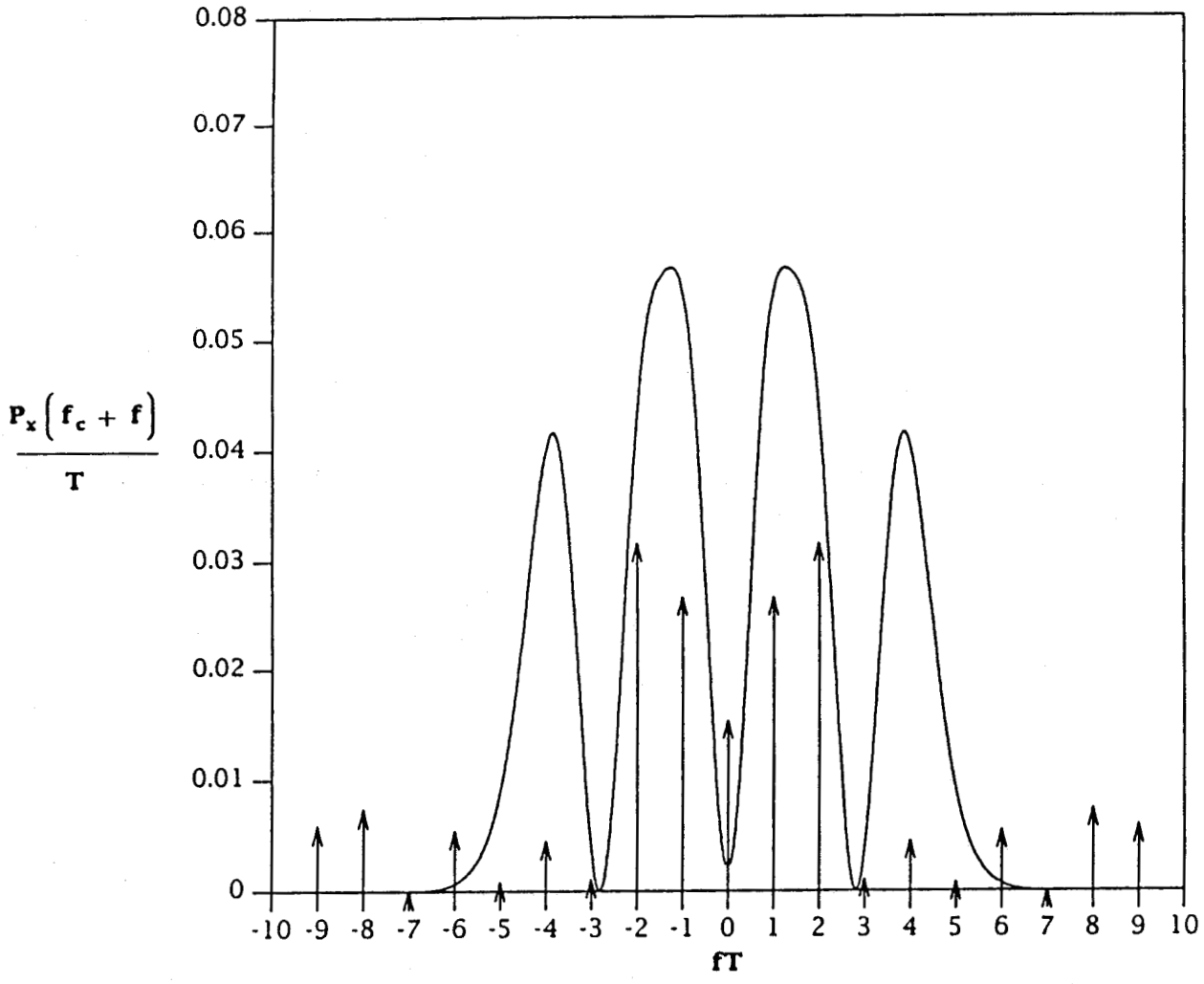

Figure 8. The continuous and discrete spectra of sine-pulse 4FSK for modulation index k = 2.

Appropriate Bessel function tables, such as those of the British Association for the Advancement of Science (1950), help to evaluate (40) for a useful range of k values. For k=2 one obtains a total discrete power of approximately 0.194, or a 38.8 percent power content for the aggregate of all spectral lines.

Figure 9 illustrates the asymptotic behavior of this sine pulse, k=2, continuous-phase 4FSK. The scales are logarithmic. Because the assumed sine pulse is continuous everywhere, while its derivative is not, the slope must be -6 asymptotically for very large fT. The actual computed peak envelope agrees with $(5/32)(fT)^{-6}$, which is analytically deduced from (39).

5. SPECTRA FOR 4FSK WITH RAISED-COSINE WAVEFORMS

The raised cosine (or squared sine pulse) parent waveform with modulation index k is

$$h(t) = (k/2T)(1-\cos(2\pi t/T)) \qquad \text{for } 0 \leq t \leq T. \tag{41}$$

From now on, k is assumed to be an even integer for this raised cosine pulse. Next,

$$q(t)] = e^{j(k/2)\Delta]} \bullet (2\pi t/T - \sin(2\pi t/T)) \quad , \tag{42}$$

which by setting $\tau=T$ and modifying (35) (see Appendix C) to read

$$e^{jz\sin\theta} = \sum_{n=-\infty}^{\infty} J_n(z)e^{jn\theta}, \tag{43}$$

produces the Fourier coefficients by inspection:

$$c_n] = (-1)^{n-(k/2)\Delta]} \; J_{n-(k/2)\Delta]}((k/2)\Delta]) \quad . \tag{44}$$

It follows from (18) that

$$R(f)] = (T/\pi)e^{-j\pi fT}\sin(\pi ft) \sum_{m=-\infty}^{\infty} (-1)^m \frac{J_m((k/2)\Delta])}{fT-(m+(k/2)\Delta])} \; . \tag{45}$$

This equation differs from the corresponding result published in Rowe and Prabhu (1975). [See their equation (116), p. 1113.] In as much as repeated derivations of R(f)] all lead us to the same $(-1)^m$ after the Σ sign, we assume that an inadvertent typographical error could have occurred in the quoted BSTJ article. In what follows we adhere to the R(f)] as given in (45).

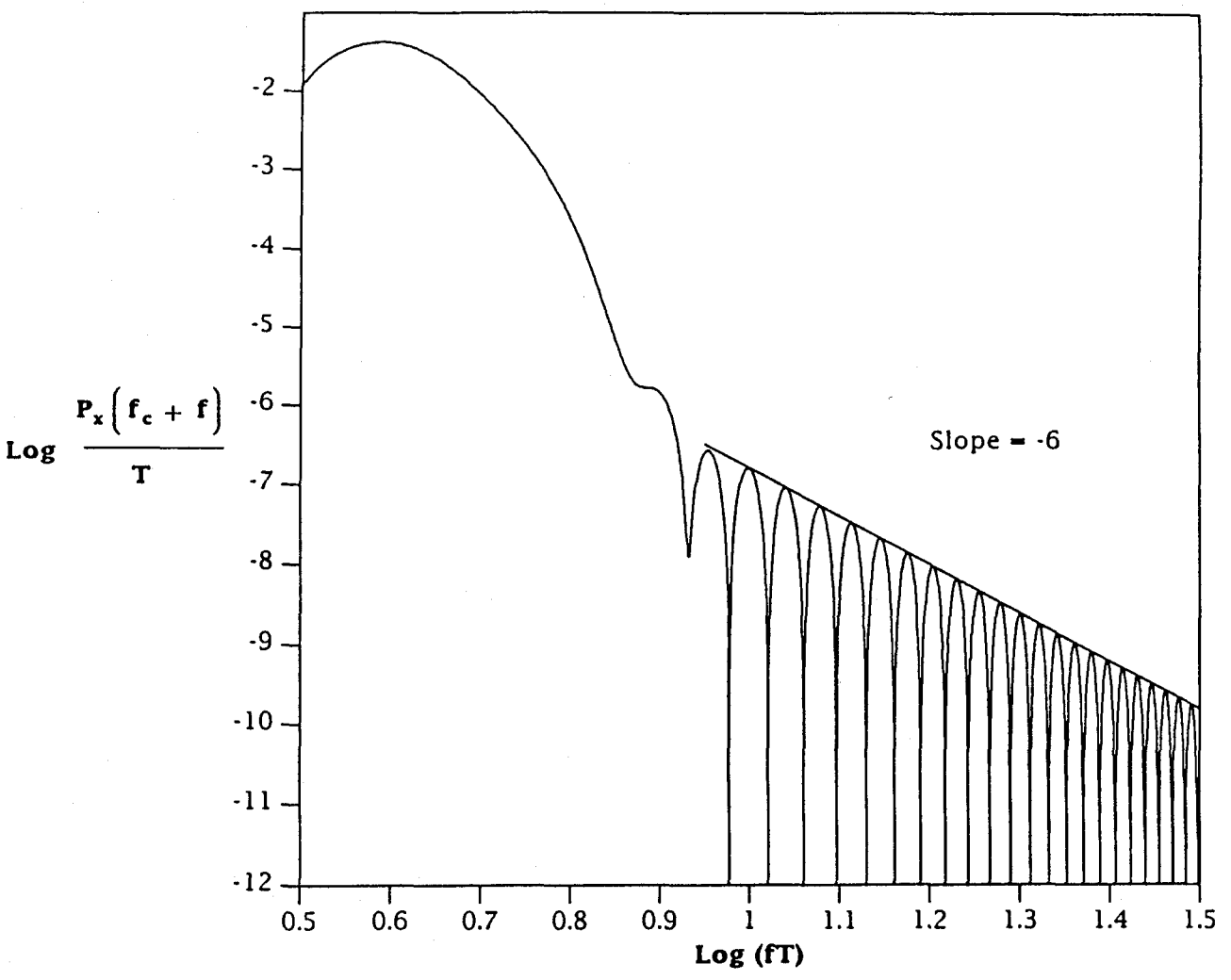

Figure 9. The asymptotic continuous spectral behavior of the k = 2, sine-pulse, 4FSK for large frequencies.

The next step is to write down a formula for the spectrum. The problem here is not difficult conceptually, but rather how best to keep track of summation indices. We propose the following scheme. Let D and S be sets of double and single integers, respectively, defined as:

$$\begin{aligned} D &= \{(1,-1),(1,3),(1,-3),(-1,3),(-1,-3),(3,-3)\} \\ S &= \{1, -1, 3, -3\}. \end{aligned} \tag{46}$$

Then, if $d=(\nu,\mu)$ denotes a double element in D and s stands for any particular single number in S, introduce two auxiliary quantities,

$$\begin{aligned} A_d(fT) &= \sum_{n=-\infty}^{\infty} (-1)^n \frac{J_{n-\nu k/2}(\nu k/2) - J_{n-\mu k/2}(\mu k/2)}{fT-n}, \\ B_n &= \sum_{s\varepsilon S} J_{n-sk/2}(sk/2). \end{aligned} \tag{47}$$

With the aid of (46) and (47), one writes the power spectrum of the raised cosine 4FSK for k an even integer:

$$\frac{P_x(f_c+f)}{T} = \frac{\sin^2(\pi fT)}{32\pi^2} \sum_{d\varepsilon D} A_d^2(fT) + (1/32) \sum_{n=-\infty}^{\infty} B_n^2\, \delta(fT-n), \tag{48}$$

where the continuous and discrete spectral components are clearly separated. This elaborate equation corresponds to the raised-cosine results presented earlier by Rowe and Prabhu (1975).

Figure 10 illustrates the total, continuous plus discrete, spectra for this raised-cosine pulse 4FSK with modulation index set at k=2. Again the axes are linear and the emphasis is on the central region of the spectrum. A local minimum with a value $(J_1(1) - J_3(3))^2/8 \cong .002$ occurs at f=0. Two nulls of the continuous spectrum seem to occur approximately at $fT=\pm 3.4$. Other nulls are possible at larger frequency deviations. The bulk of the power is contained in the $-8<fT<8$ frequency region.

As it was for the sine pulse, the discrete spectrum again consists of an infinite number of lines. The amplitudes (arrows) of the discrete lines are drawn to represent coefficients $1/32\ B_n^2$ on the ordinate scale. In some cases, when the coefficients are too small, the arrows are omitted.

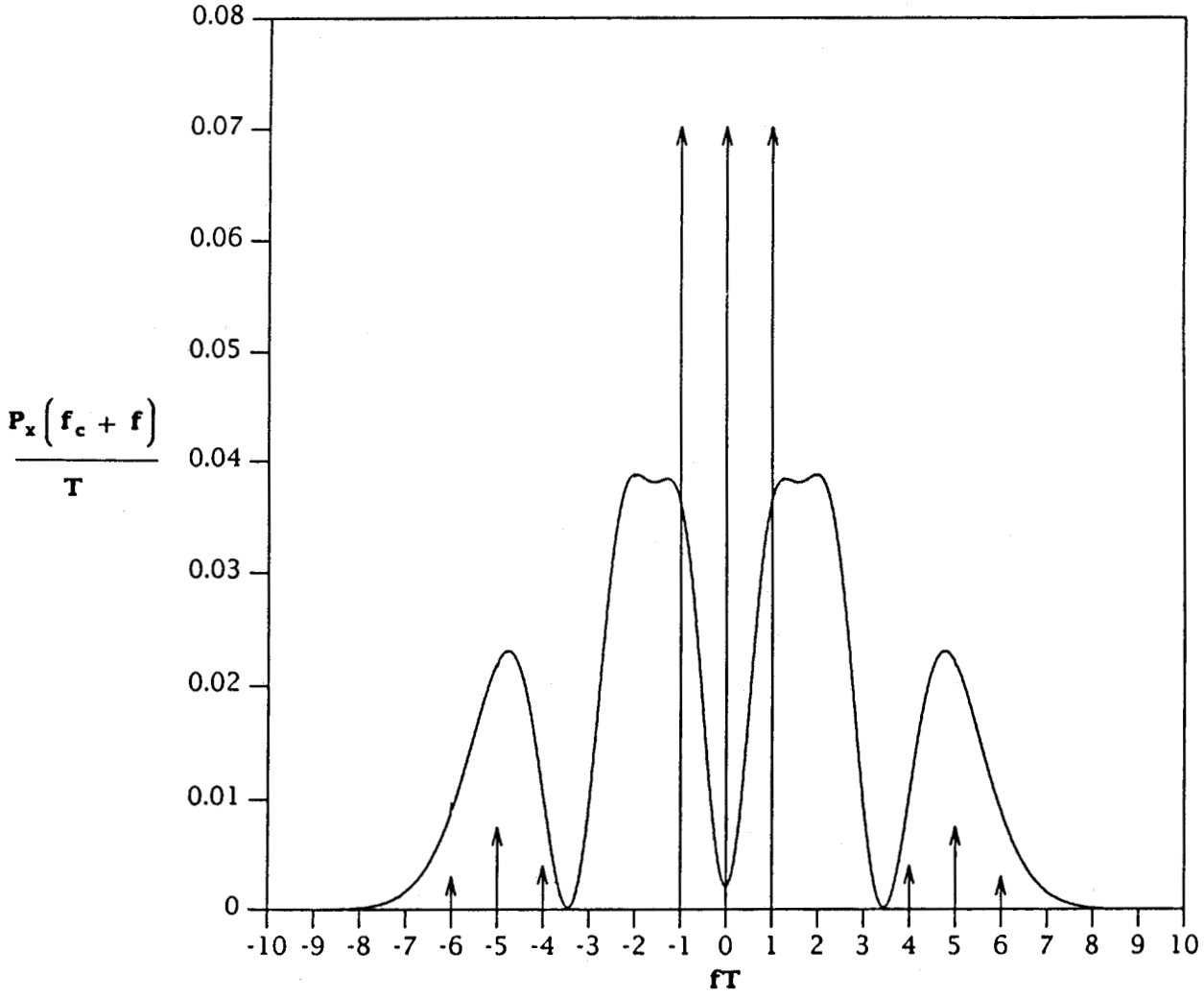

Figure 10. The continuous and discrete spectra of raised-cosine pulse 4FSK for modulation index k = 2.

Neighboring lines are separated by a frequency spacing of 1/T. For k=2 the total power in the spectral lines is

$$(1/32)\sum_{n=-\infty}^{\infty} B_n^2 = (1/16)(2+3J_2(2)+2J_4(4)+J_6(6)), \qquad (49)$$

as shown in Appendix C. Tables of Bessel functions yield a relative total discrete line power of 48.3 percent.

Figure 11 is the log-log presentation of the 4FSK spectrum, where the pulse waveforms are raised cosines and the modulation index is k=2. Because the lowest discontinuous derivative is the second derivative, the slope of the envelope must be asymptotically approaching -8 as fT tends to infinity. Equations show that the actual peak asymptote must be $(5/2\pi^2)(fT)^{-8}$.

6. SPECTRA FOR 4FSK WITH SQUARED RAISED-COSINE WAVEFORMS

The generator waveform, for what we choose to call the "squared raised-cosine" 4FSK with modulation index k, is

$$h(t) = (k/3T)(1-\cos(2\pi t/T))^2 \qquad \text{for } 0 \le t \le T. \qquad (50)$$

Its 4FSK baseband vector (see (11) above) is then

$$q(t)] = e^{j(k/12)\Delta]\bullet(12\pi t/T-8\sin(2\pi t/T)+\sin(4\pi t/T))}. \qquad (51)$$

This is apparently a more complicated case than the sine pulse and the raised-cosine pulse cases studied in the two previous sections. To simplify, assume k=2 for this squared raised-cosine waveform.

As we have done before, let τ=T and expand q(t)] in Fourier series with coefficients $c_n]$ (see (14) and (15) above). This expansion is rather involved. Its details are delegated to Appendix C. The result is

$$c_n] = I_{n-\Delta]}(-(4/3)\Delta],(1/6)\Delta]), \qquad (52)$$

where for integer valued n and real numbers u and v, the function $I_n(u,v)$ is defined to be

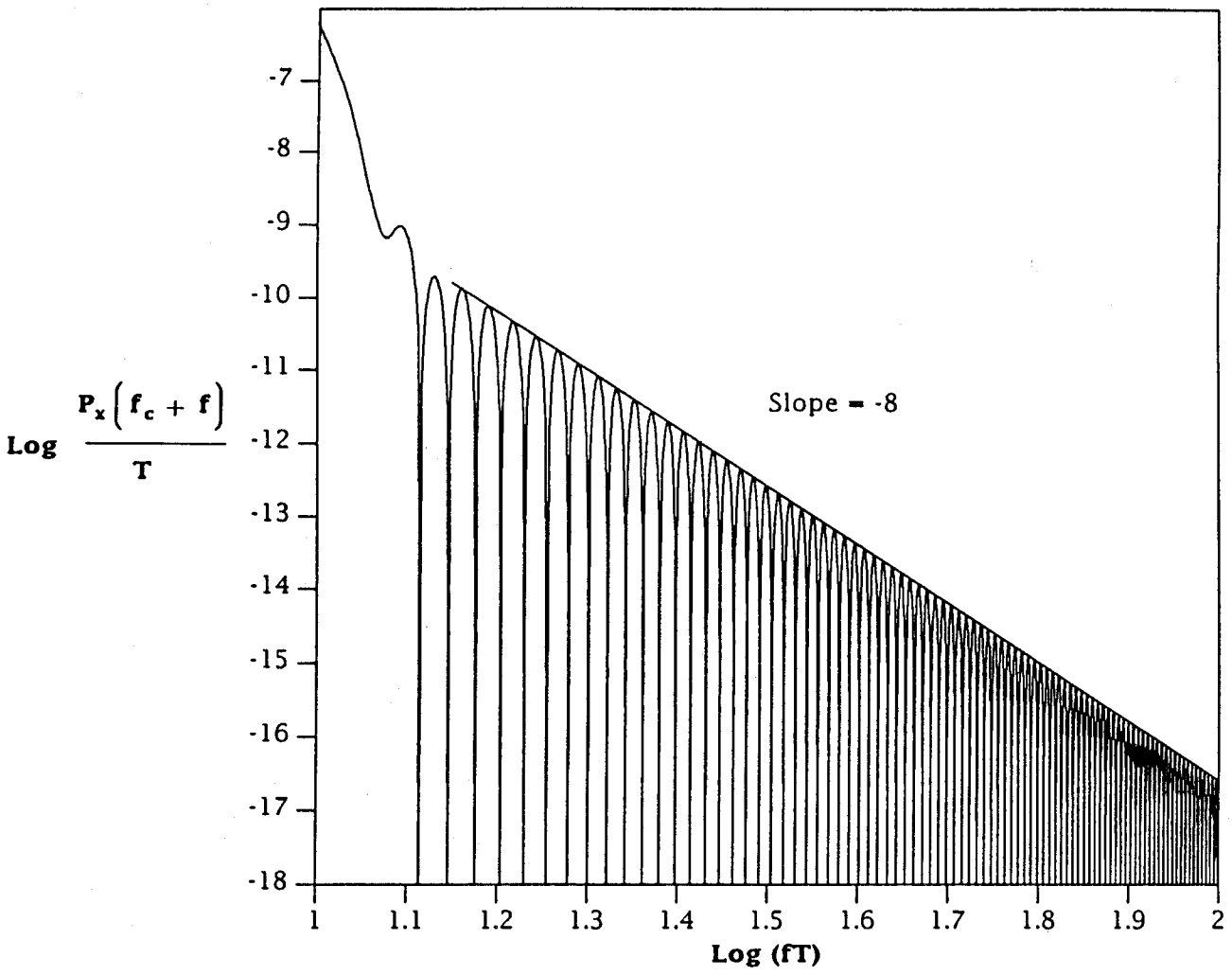

Figure 11. The asymptotic continuous spectral behavior of the k = 2, raised-cosine pulse, 4FSK for large frequencies.

$$I_n(u,v) = \sum_{m=-\infty}^{\infty} J_{n-2m}(u)J_m(v)$$
$$= (1/\pi) \int_0^{\pi} \cos(u\sin\theta + v\sin 2\theta - n\theta)d\theta. \quad (53)$$

Appendix C offers proofs and several other expressions for this indexed, bi-variate function $I_n(u,v)$. For computational purposes, either of the two forms in (53) can be used. If fast subroutines are readily available for $J_n(x)$, a truncated version of the infinite series of (53) may work. Otherwise, rapidly converging quadrature techniques can benefit from the second part of (53).

Let

$$A_{n,m} = I_{n-1}(-4/3,1/6)\ I_{m-1}(-4/3,1/6) + I_{n+1}(4/3,-1/6)\ I_{m+1}(4/3,-1/6)$$
$$+ I_{n-3}(-4,1/2)\ I_{m-3}(-4,1/2) + I_{n+3}(4,-1/2)\ I_{m+3}(4,-1/2)$$
and (54)
$$B_n = I_{n-1}(-4/3,1/6) + I_{n+1}(4/3,-1/6) + I_{n-3}(-4,1/2) + I_{n+3}(4,-1/2).$$

Then the power spectrum for the k=2, squared raised-cosine, 4FSK is given by

$$\frac{P_X(f_c+f)}{T} = \frac{\sin^2(\pi fT)}{32\pi^2} \sum_{n,m=-\infty}^{\infty} \frac{4A_{n,m}-B_nB_m}{(fT-n)(fT-m)} +$$
$$+ (1/32) \sum_{n=-\infty}^{\infty} B_n^2\, \delta(fT-n). \quad (55)$$

The first half of this equation is the continuous spectral component. The second half is the line spectrum.

Figure 12 shows the main central region of the composite spectrum (55) for the postulated continuous-phase, no overlap, k=2 4FSK with squared raised-cosine waveforms. The coordinate axes are linear. The continuous spectrum does not have nulls in the region indicated, although there are pronounced

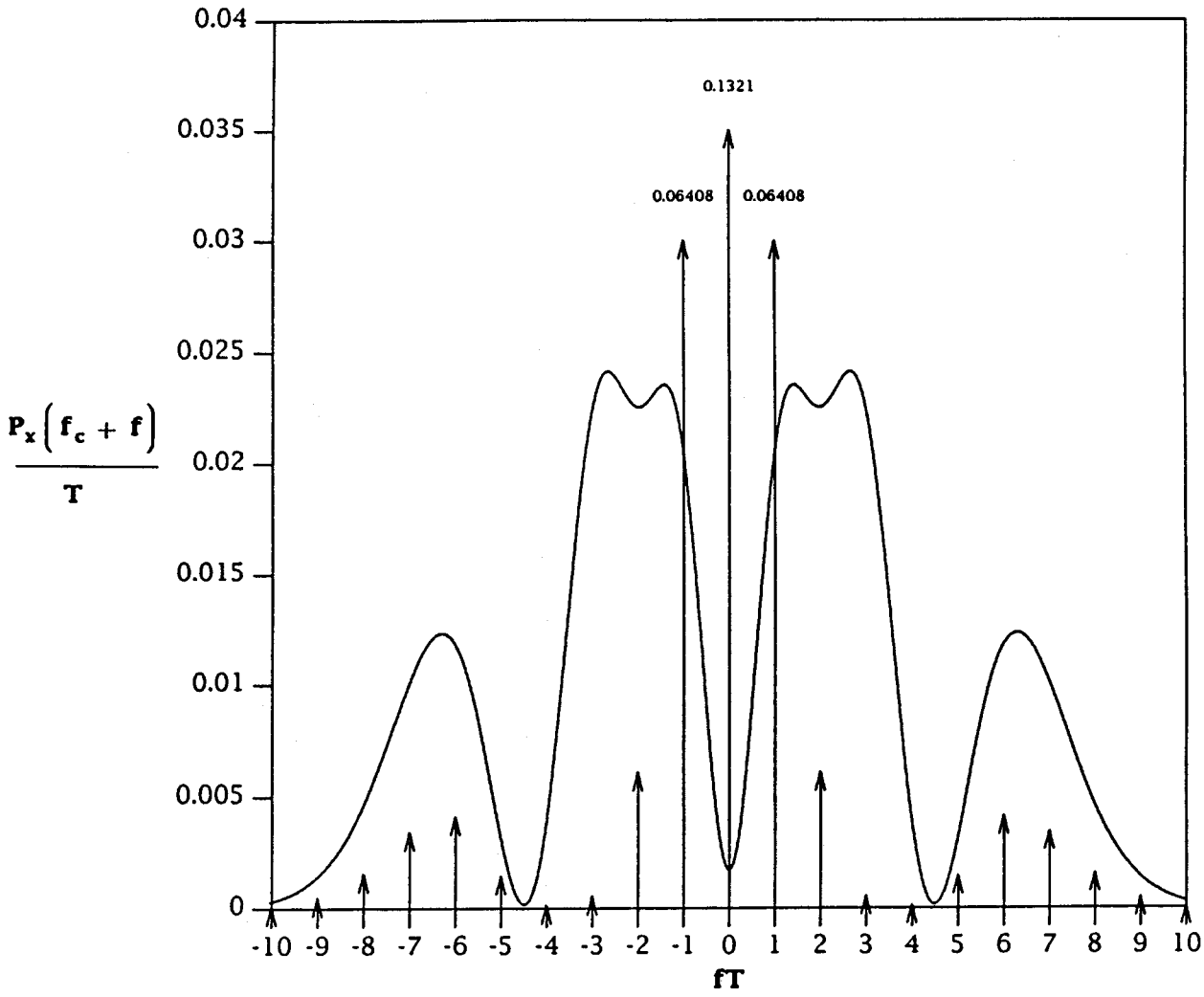

Figure 12. The continuous and discrete spectra of squared raised-cosine pulse 4FSK for modulation index k = 2.

minima at fT=0 and ±4.5. The main signal power is contained within -10<fT<10.

The discrete spectrum consists of infinitely many equi-distant lines, spaced 1/T Hz apart. The total power in the discrete spectral lines is .296 or 59.2 percent, as can be computed from the identity

$$\sum_{n=-\infty}^{\infty} B_n^2 = 2\left[2+3I_2\left(\frac{8}{3},-\frac{1}{3}\right)+2I_4\left(\frac{16}{3},-\frac{2}{3}\right)+I_6\left(8,-1\right)\right]. \qquad (56)$$

The proof of (56) follows from the generalized form of the Neumann Addition Theorem, given in Appendix C for the $I_n(u,v)$ functions.

Figure 13 is a logarithmic representation of the continuous spectrum. Emphasis is on large fT values. Because for the squared raised-cosine pulse, the lowest discontinuous derivative is the fourth derivative, the asymptotic slope of the power spectrum should be $(40/\pi^2)(fT)^{-12}$, as predicted from (55).

7. BACKGROUND AND SPECTRA FOR BINARY SQUARE-WAVE FSK

The binary, or M=2, FSK has probably received the most attention in the past. To summarize it in the present vector context, a large portion of the equations derived above remains valid. With the understanding that two-dimensional

$$\Delta] = \begin{pmatrix} 1 \\ -1 \end{pmatrix}$$

$$[M] = \frac{1}{4}\begin{pmatrix} 1 & -1 \\ -1 & 1 \end{pmatrix} \qquad (57)$$

$$w] = \frac{1}{2}\,1]$$

are to be used, earlier (11), (14) to (18), the first part of (19), and (21) to (24) all remain valid for arbitrary integer-valued modulation index k. The discrete spectrum exists.

Case for k=1

Set τ=2T and note that the Fourier coefficient $c_n]$ satisfies (24). But then the R(f)] vector function must be as defined in (26). Substitution in earlier (19) and (21) yield the continuous and discrete baseband spectra. Another substitution into (4) and (5) produce the desired spectrum at radio frequency.

The total, continuous plus discrete, spectral density for the phase-continuous, square-pulse, 2FSK with modulation index k-1 is

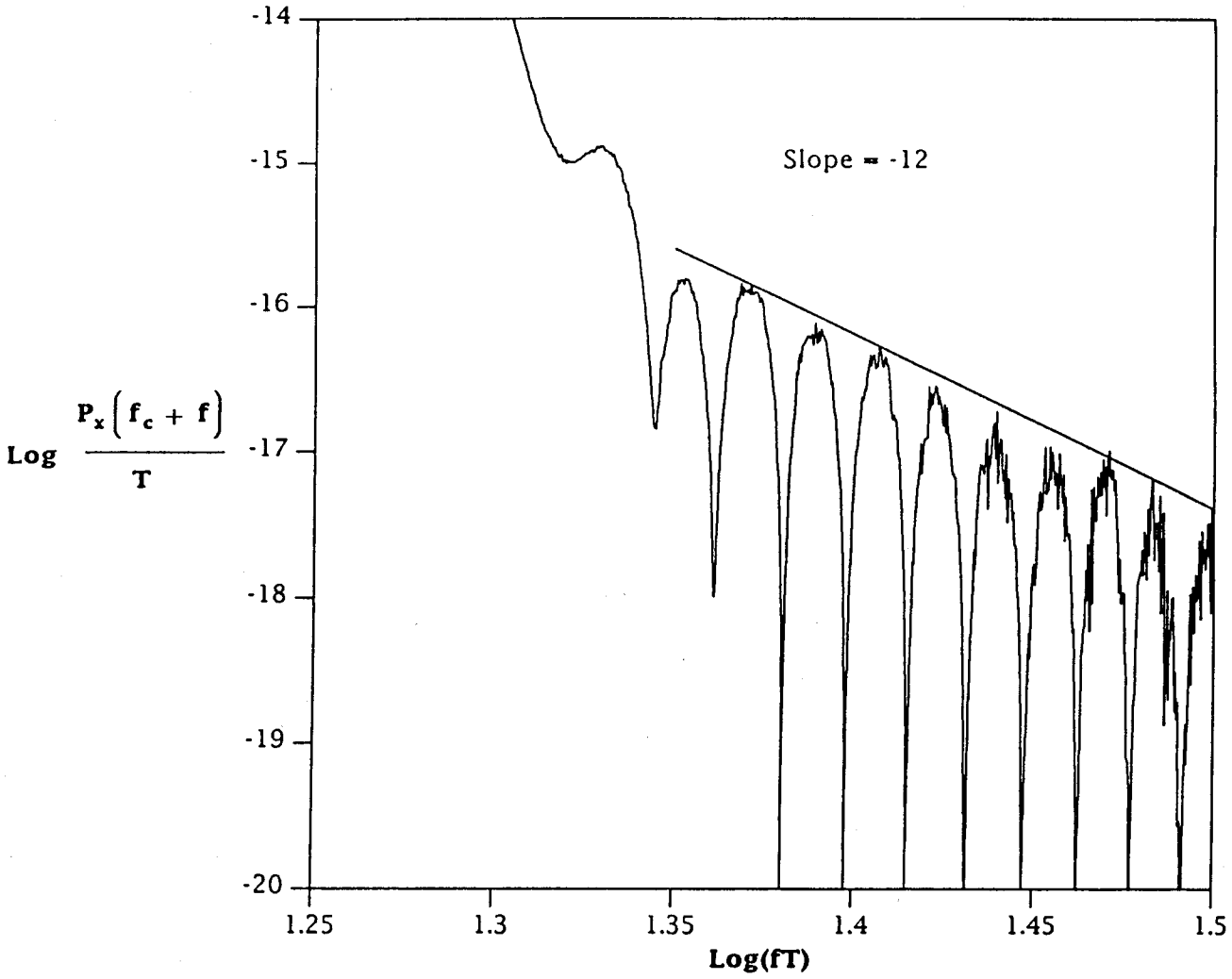

Figure 13. The asymptotic continuous spectral behavior of the k = 2, squared raised-cosine, 4FSK for large frequencies.

$$\frac{P_x(f_c+f)}{T} = \frac{\cos^2(\pi fT)}{8\pi^2(f^2T^2-1/4)^2} + \frac{1}{8}\,(\delta(fT-1/2) + \delta(fT+1/2)). \qquad (58)$$

The first half of this equation is the continuous power spectral density. The second half is the discrete component. This result was apparently first derived by Bennett and Rice (1963), later by Anderson and Salz (1965), and others.

The 2FSK, k=1, spectrum is plotted in Figure 14. The display is linear in both coordinates. The region around fT=0 is emphasized. Centered on fT=0 is the single symmetric peak of the continuous part. The nulls occur at fT=±3/2, ±5/2, ±7/2, and so forth. The spacing between adjacent nulls in Figure 14 is generally one fT unit, except at the origin where that spacing is three units.

There are two discrete lines shown. They occur at fT=±1/2 and their individual power content is 1/8. This is the same power as contained in the continuous spectrum (see Appendix B for details of needed integration). Thus the total line power is 50 percent of the total FSK power.

Figure 15 displays the continuous binary FSK spectrum on a logarithmic scale. For large fT values the predicted peak asymptotic envelope is $(1/8\pi^2)(fT)^{-4}$. That fact is quite as expected, because the elementary waveform h(t) is discontinuous.

Case for k=2

Set τ=T and use the Fourier coefficient c_n] of (24). The R(f)] is of the same form as given above in (28).

The spectral density for the phase-continuous, square-pulse, binary FSK with modulation index k=2 follows again by the same substitution process:

$$\frac{P_x(f_c+f)}{T} = \frac{\sin^2(\pi fT)}{2\pi^2(f^2T^2-1)^2} + \frac{1}{8}\,(\delta(fT-1) + \delta(fT+1)). \qquad (59)$$

This formula illustrates the, by now quite familiar, continuous and discrete components of the spectral density. The same result has been previously derived by Bennett and Rice (1963), Anderson and Salz (1965), and others.

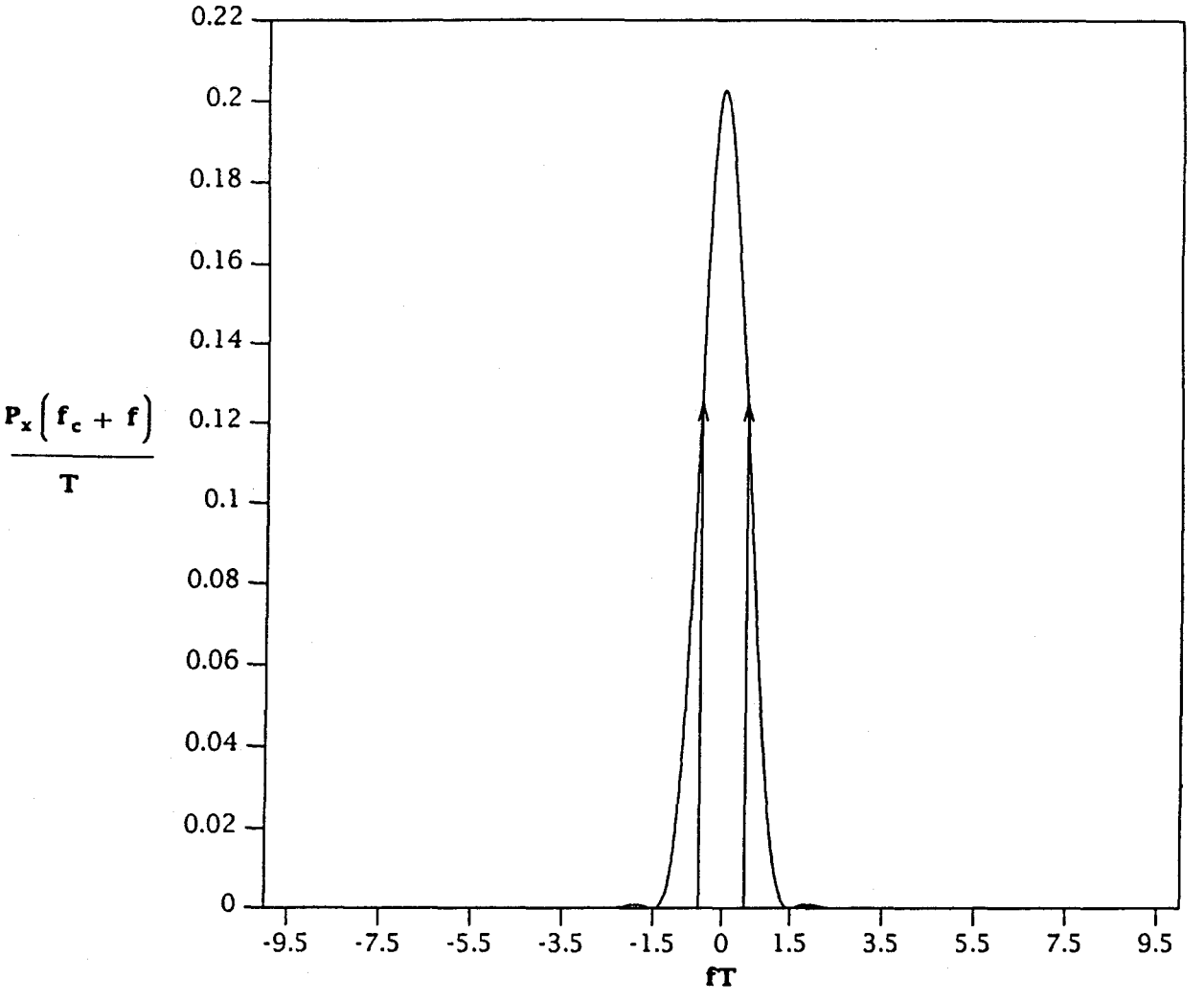

Figure 14. The continuous and discrete spectra of square-wave 2FSK for modulation index k = 1.

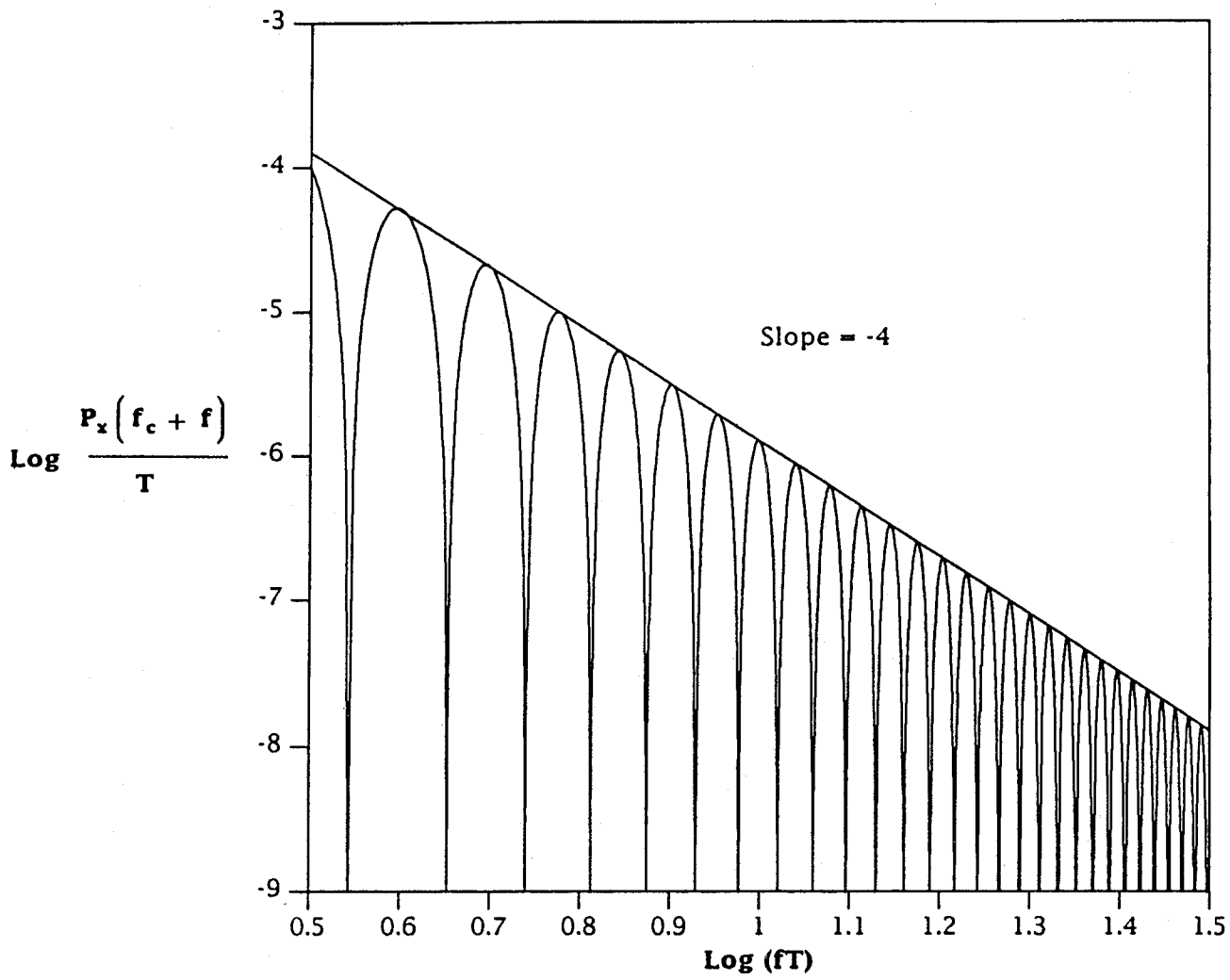

Figure 15. The asymptotic continuous spectral behavior of the k = 1, square-wave, 2FSK for large frequencies.

Figure 16 illustrates the central part of this power spectrum. Both coordinate axes are linear. Notice that the continuous component has two prominent peaks at fT=±1. Thus, there are no nulls at ±1, but there are nulls at all other positive and negative integers.

Two discrete spectral lines coincide with the continuous peaks, as they are also located at fT=±1. Just like in the k=1 case, the power content of each line is 1/8. The total power of the two continuous peaks equals 1/4, as is seen from the integrals in Appendix B. Thus, the discrete spectrum again contains 50 percent of the total binary FSK power.

Figure 17 shows the asymptotic behavior of the k=2 2FSK for the assumptions cited above. The horizontal and vertical scales are both logarithmic. As fT tends to infinity, the predicted asymptotic slope is given by $(1/2\pi^2)(fT)^{-4}$.

8. SPECTRUM FOR BINARY FSK WITH SQUARED RAISED-COSINE WAVEFORMS

Binary FSK, or 2FSK, is perhaps the most studied case of FSK systems with different waveforms (see Bennett and Rice, 1963; Anderson and Salz, 1965; and elsewhere). In this section, the apparently less familiar waveform of squared raised-cosine (or its equivalent sine-pulse to the fourth power) is presented. The formulas follow immediately from earlier derivations of Sections 6 and 7.

The parent waveform h(t) is the same as in (50). Assuming that Δ] and [M] are as defined in (57), that the mod-index k=2, and that one denotes u=-4/3 and v=1/6, the power spectrum is given by

$$\frac{P_x(f_c+f)}{T} = \frac{\sin^2(\pi fT)}{8\pi^2} \sum_{n=-\infty}^{\infty} \left(\frac{I_{n-1}(u,v) - I_{n+1}(-u,-v)}{fT-n} \right)^2 + (1/8) \sum_{n=-\infty}^{\infty} (I_{n-1}(u,v) + I_{n+1}(-u,-v))^2 \delta(fT-n), \tag{60}$$

where $I_n(u,v)$is the function defined earlier in (53).

Figure 18 shows the central parts of the continuous and discrete spectra of this squared raised-cosine pulse 2FSK. Note that there are two main maxima at fT=±1.5 and a null at fT=0. Other nulls are not only possible, but do occur at higher values of fT, such as for fT ≧ 12.

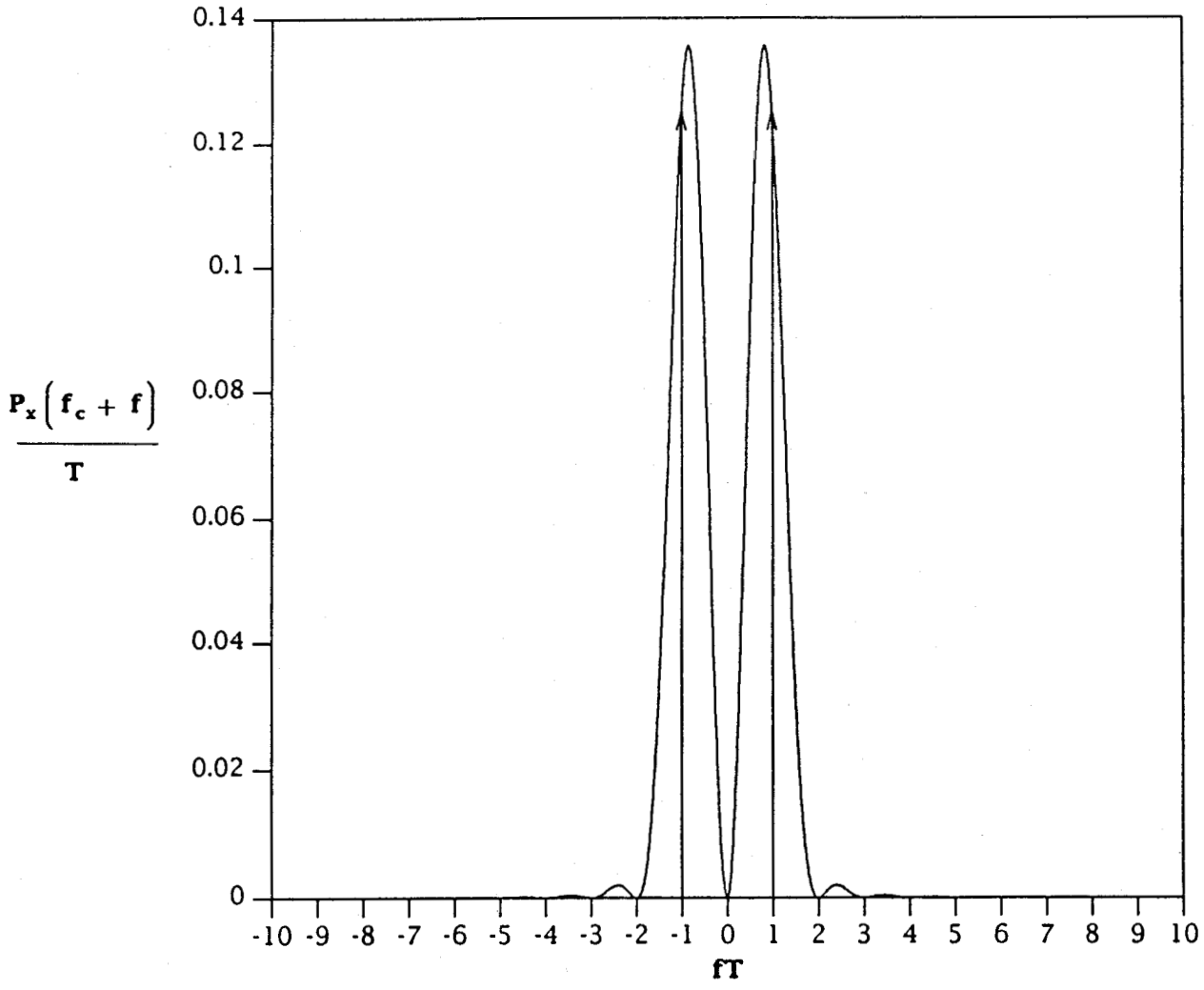

Figure 16. The continuous and discrete spectra of square-wave 2FSK for modulation index k = 2.

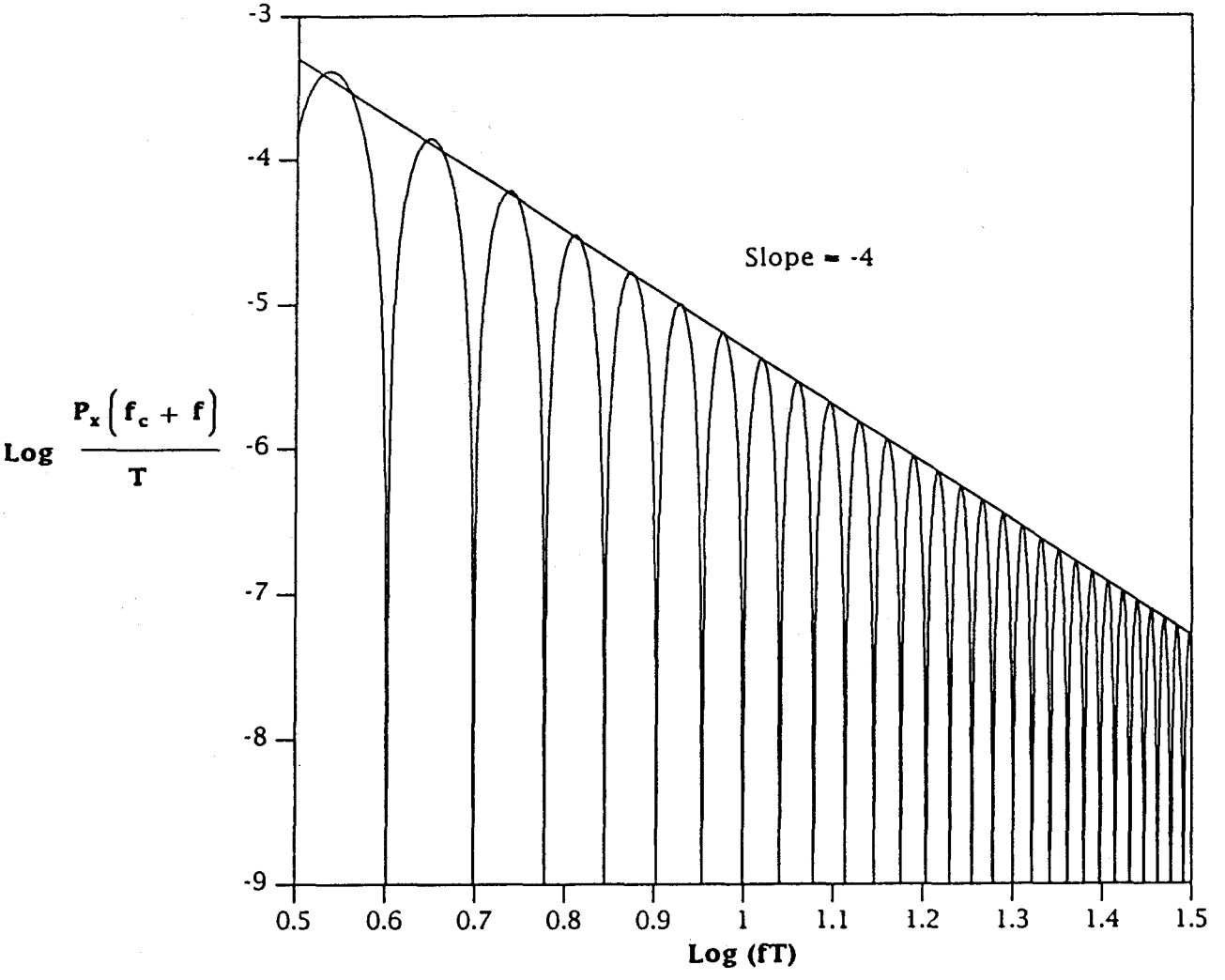

Figure 17. The asymptotic continuous spectral behavior of the k = 2, square-wave, 2FSK for large frequencies.

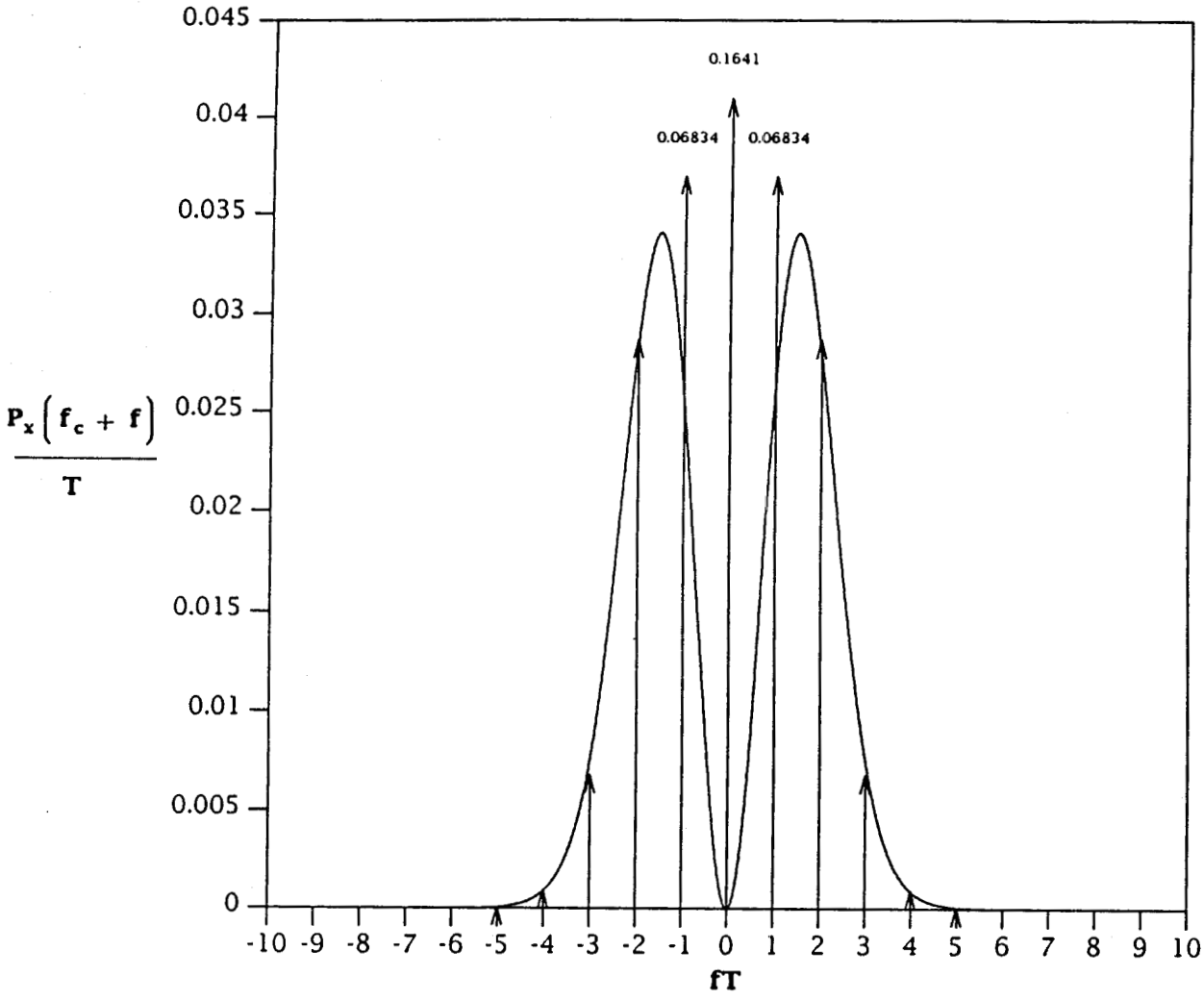

Figure 18. The continuous and discrete spectra of squared raised-cosine pulse 2FSK for modulation index k = 2.

As observed for the 4FSK with the identical parent waveform, and as follows from the second half of (60), the discrete spectrum contains an infinite number of lines. The amplitudes of the three central lines exceed the vertical scale. Their values are indicated in Figure 18 numerically, such as by 0.1641 at fT=0. These lines occur at all integer values of fT. For the assumed modulation index of k=2, the total power in the line spectrum is estimated to be 0.374. That amounts to 74.8 percent of the total signal power. This number is deduced from either side of the identity,

$$\sum_{n=-\infty}^{\infty} (I_{n-1}(u,v) + I_{n+1}(-u,-v)^2 = 2(1 + I_2(-2u,-2v)). \qquad (61)$$

Just as in the case of the corresponding identity (56) for 4FSK, the justification of (61) depends on the extension of Neumann series from Bessel functions to the $I_n(u,v)$ functions.

Figure 19 is a log-log plot of the 2FSK continuous spectrum, where k=2, and the pulse shapes are squared raised-cosines. Because the lowest discontinuous derivative is the fourth, the slope of the asymptote must become -12 as fT increases. The exact value of the predicted peak asymptote is $(8/\pi^2)(fT)^{-12}$.

9. SPECTRUM FOR THE ALTERNATE-PAIR 4FSK SCHEME PROPOSED BY ROCKWELL/COLLINS

Assume a modulation format, where M=4 frequencies are keyed with certain restrictions that alternate from one T-interval to the next. An example is a scheme proposed by Rockwell/Collins, where in even numbered intervals one has a binary square-wave choice of $\pm f_1$, and in odd numbered intervals a different binary square-wave choice of $\pm 3f_1$. Here f_1 can be any assigned frequency deviation from the carrier frequency, including the particular Hz values implemented by Rockwell/Collins.

One could treat $+f_1$ as a generating pulse in each (0,T) interval, but that would destroy the premise of statistical independence between pulses. It would invalidate the entire theoretical framework assumed in previous sections (Prabhu and Rowe, 1974). A second option is to combine successive intervals, such as (0,T) and (T,2T) into one "super-interval" (0,2T). The super-interval carries 2 bits, as is usual for 4FSK. The 2T-approach has the unfortunate side effect that the formulas become longer and more complicated.

We follow the second approach. Let the modulation index be simply defined as $2f_1T$ and assume that its value is k=2. Furthermore, let

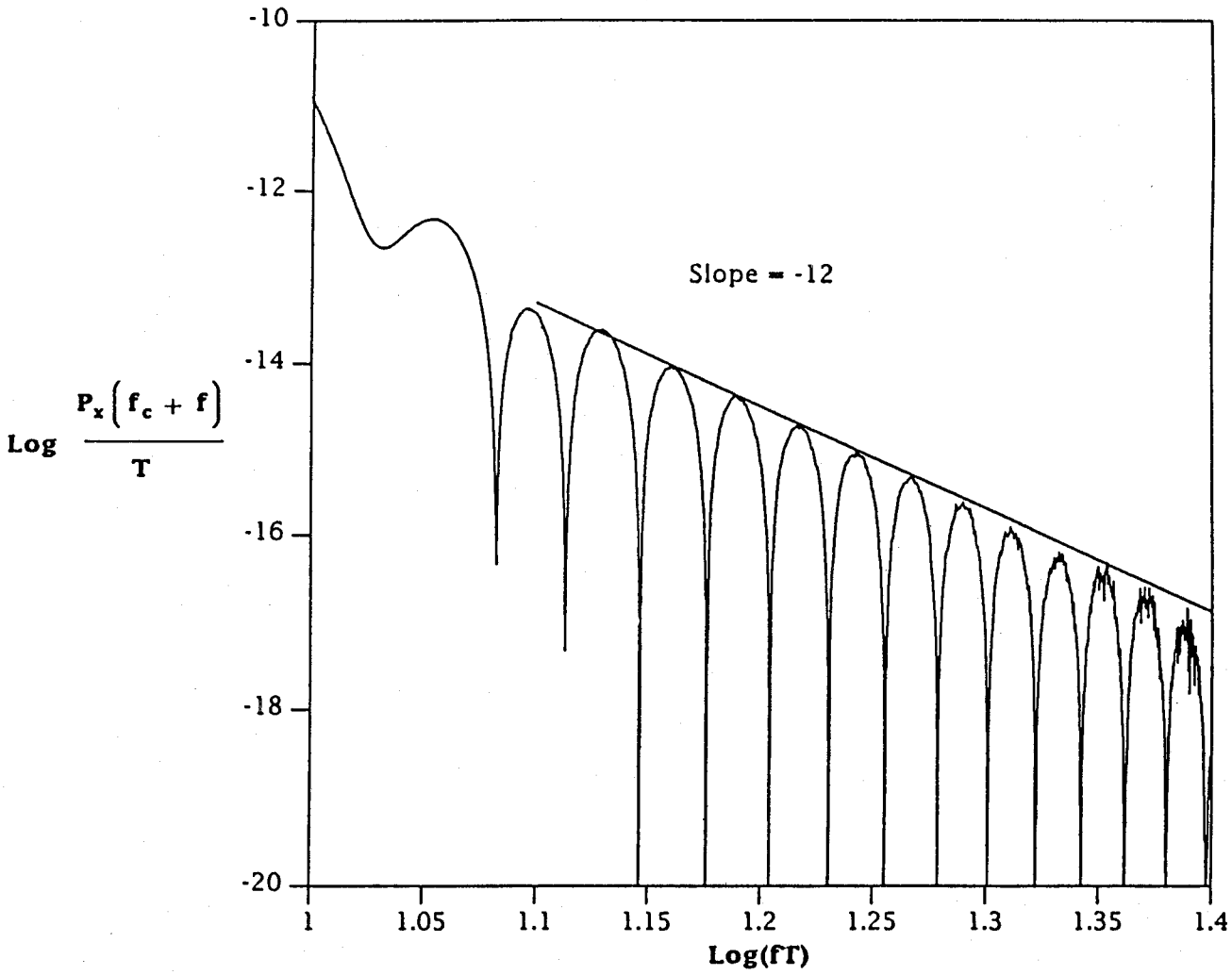

Figure 19. The asymptotic continuous spectral behavior of the k = 2, squared raised-cosine, 2FSK for large frequencies.

$$h(t) = 1/T \qquad \text{for } 0<t\leq T\ ,$$
$$= 0 \qquad \text{elsewhere,} \tag{62}$$

and define two vectors

$$\Delta] = \begin{pmatrix} 1 \\ -1 \end{pmatrix},$$
$$\Delta'] = \begin{pmatrix} 3 \\ -3 \end{pmatrix}. \tag{63}$$

Then the waveform vector (compare with (9)) for a pulse in the (0,2T) interval can be expressed as a direct-product type of function of the two vectors:

$$h(t)] = \Delta] \bullet h(t) \qquad \text{for } 0<t\leq T,$$
$$= \Delta'] \bullet h(t-T) \qquad \text{for } T<t\leq 2T. \tag{64}$$

The corresponding baseband vector, see earlier (11), now becomes

$$q(t)] = e^{j2\pi\Delta]} \bullet t/T \qquad \text{for } 0<t\leq T,$$
$$= e^{j2\pi\Delta'] } \bullet t/T \qquad \text{for } T<t\leq 2T, \tag{65}$$

and the probability vector w] is the same as in (12) for the (0.2T) interval.

The discrete line spectrum exists. The Fourier integral transform R(f)] may be computed directly, without a need for a Fourier series expansion:

$$R(f)] = \int_0^{2T} q(t)]\ e^{-j2\pi ft} dt$$
$$= \frac{T}{j2\pi}(1-e^{-j2\pi fT})\left(\frac{1}{fT-\Delta]} + \frac{e^{-j2\pi fT}}{fT-\Delta']}\right). \tag{66}$$

To compute the spectrum, the earlier (19) and (21) are still valid. In (21) one must set $\tau=2T$. That permits, at least in principle, the existence of $\delta(fT-n/2)$ for any, odd or even, integer valued n. To simplify, introduce the abbreviation

$$C_m = \frac{m+1/2}{(m+7/2)(m+3/2)(m-1/2)(m-5/2)}\ . \tag{67}$$

Then, after a long and careful substitution of (66) into (19) and (21), one obtains the power spectral density for the continuous-phase, no overlap, one bit per T, Rockwell/Collins type of 4FSK with modulation index k=2:

$$\frac{P_x(f_c+f)}{T} = \frac{\sin^2(\pi fT)}{4\pi^2}\left[\frac{1}{(f^2T^2-1)^2} + \frac{9}{(f^2T^2-9)^2}\right] + (1/32)\left[\delta(fT-1) + \delta(fT+1) + \delta(fT-3) + \delta(fT+3)\right] + \frac{8}{\pi^2}\sum_{m=0}^{\infty} C_m^2\left[\delta(fT-m-1/2) + \delta(fT+m+1/2)\right] . \quad (68)$$

This equation consists of three parts. The first part is the continuous spectral density. The remaining two parts show two distinct line spectra. The middle term represents the periodicity inherent in the underlying 1/T keying format. The third term shows an infinite set of spectral lines that decays as $1/f^6$ with increasing frequency. Its presence appears to be due to the alternating-interval constraint introduced above.

Figure 20 illustrates the central region of the total power spectrum in (68). Both coordinate axes are linear. The continuous component has four prominent peaks at fT=±1 and ±3. The nulls occur at integer values of fT. They are separated by two fT units in the central interior region and by one fT unit in both exterior regions.

The two families of the discrete lines are quite different. First, the four major delta functions, each of power 1/32, coincide with the four continuous peaks. That feature of the alternating Rockwell/Collins waveforms agrees with the plain square-wave 4FSK for k=2 (see Figure 4). The rest of the line spectrum is new. The new lines occur at all fT values that happen to be odd multiples of 1/2.

The power in the two terms (or four peaks) of the continuous spectrum adds up to 1/4. This is seen from the definite trigonometric integrals in Appendix B. The power in the four lines, at 1/32 per line, totals another 1/8. That leaves the rest, or 1/8, for the infinite sum of delta functions with the C_m^2 coefficients. The conclusion is that the total of the composite discrete line spectrum is 50 percent of the total 4FSK power. Noteworthy, such a 50 percent line spectrum ratio is rather typical of 2FSK systems (see Section 7).

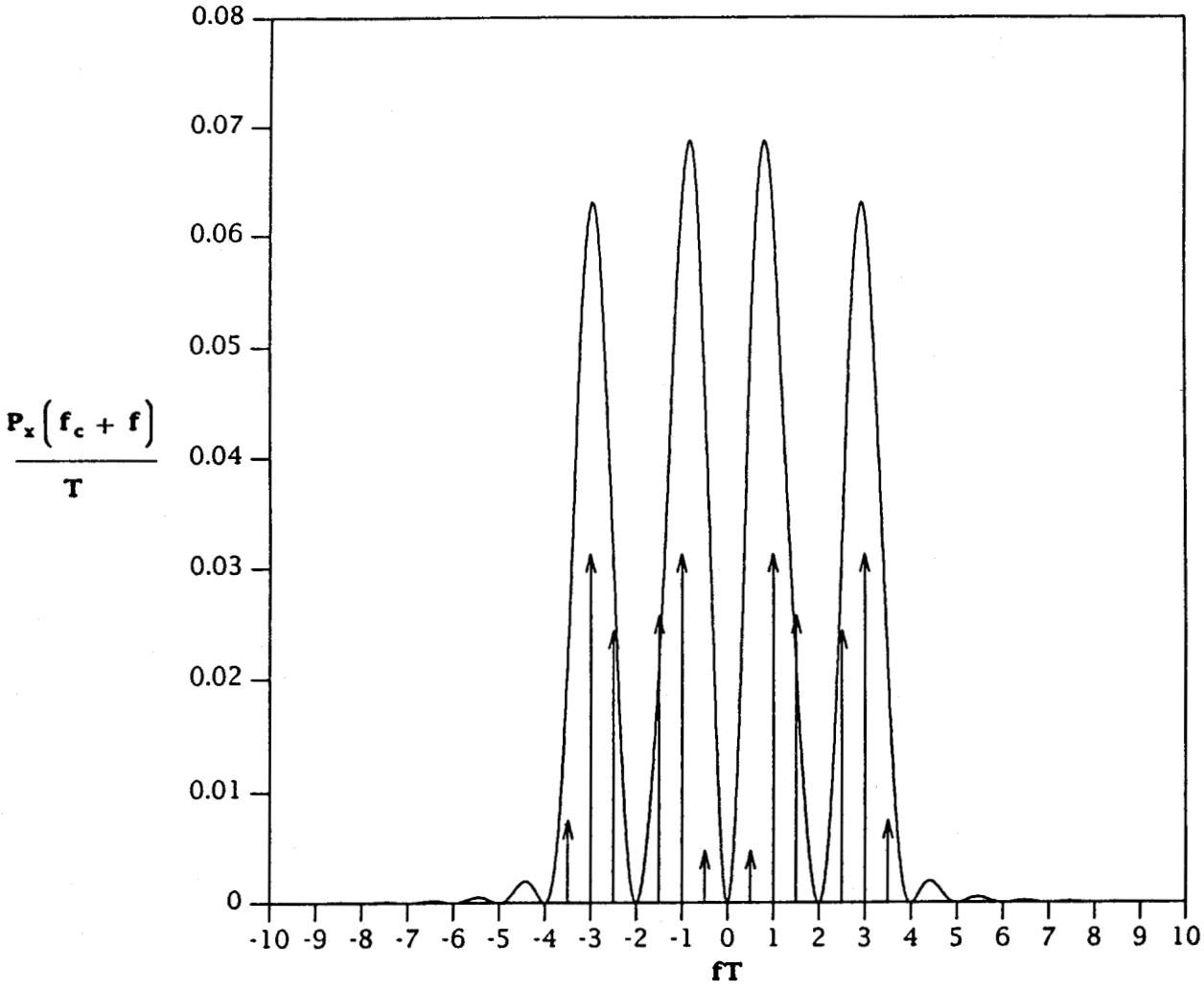

Figure 20. The continuous and discrete spectra of the alternating, square-wave pulse, 4FSK scheme proposed by Rockwell/Collins.

Figure 21 shows the asymptotic behavior of this, so called 4FSK, with alternating waveform pairs. Both coordinate axes are logarithmic. As fT increases beyond all bounds, the slope of the peak envelope must tend to minus four. The exact peak asymptote is given by $(5/2\pi^2)(fT)^{-4}$.

10. SPECTRUM FOR THE 8FSK PROPOSED BY MITRE/HARRIS

The 8FSK considered here is a digital modulation with M=8 square-wave pulses. It is also called the 8-ary or octal FSK. In a recent joint venture by MITRE and Harris Corporations, a continuous-phase 8FSK system of this general type has been proposed for a National automated system standard.

After the formal framework development for the 4FSK and 2FSK systems (see Sections 2 to 7), the extension to 8FSK spectra is straightforward. It seems that the biggest problem is how best to write 8-dimensional vectors and matrices. Vector $\Delta]$ has the equivalent transpose representation,

$$\Delta]^t = (1, -1, 3, -3, 5, -5, 7, -7). \tag{69}$$

Matrix [M] that corresponds to (20) is now

$$[M] = (1/64) \begin{pmatrix} 7 & -1 & -1 & -1 & -1 & -1 & -1 & -1 \\ -1 & 7 & -1 & -1 & -1 & -1 & -1 & -1 \\ -1 & -1 & 7 & -1 & -1 & -1 & -1 & -1 \\ -1 & -1 & -1 & 7 & -1 & -1 & -1 & -1 \\ -1 & -1 & -1 & -1 & 7 & -1 & -1 & -1 \\ -1 & -1 & -1 & -1 & -1 & 7 & -1 & -1 \\ -1 & -1 & -1 & -1 & -1 & -1 & 7 & -1 \\ -1 & -1 & -1 & -1 & -1 & -1 & -1 & 7 \end{pmatrix} \tag{70}$$

Assume k=2 and set τ=T. Then all the results for even k, up to and including (28) for R(f)], apply here. For the derivation of the final spectral expression, a lengthy and detailed substitution remains to be carried out. To do so, define a set S of integers:

$$S = \{\pm 1, \pm 3, \pm 5, \pm 7\}. \tag{71}$$

Then the power spectral density for the phase-continuous, square-wave pulse, 8FSK with modulation index k=2 is

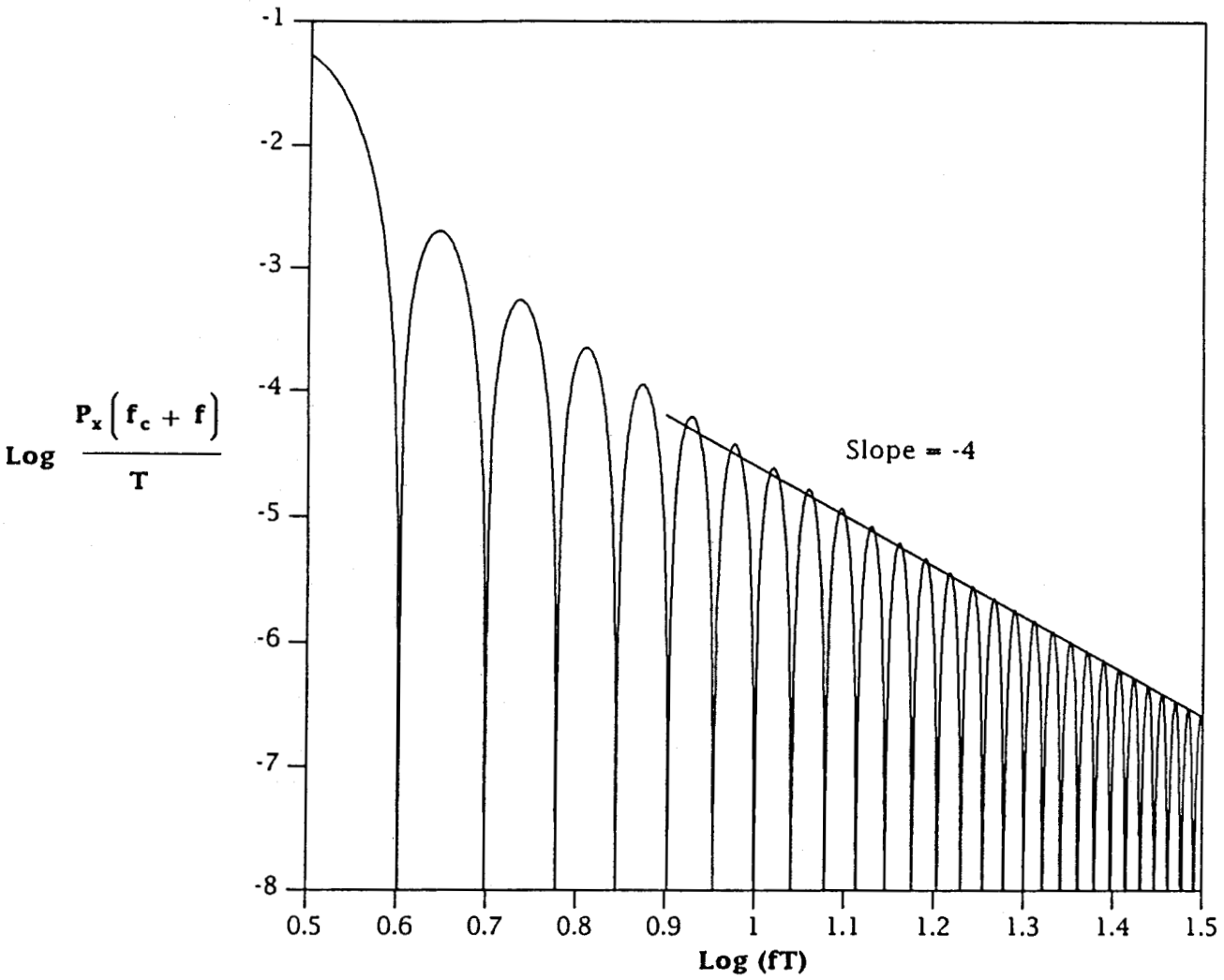

Figure 21. The asymptotic continuous spectral behavior of the k = 2, alternating square-wave pulse, 4FSK scheme proposed by Rockwell/Collins.

$$\frac{P_x(f_c+f)}{T} = \frac{\sin^2(\pi fT)}{128\pi^2}\left[8\sum_{n\epsilon S}\frac{1}{(fT-n)^2} - \left(\sum_{n\epsilon S}\frac{1}{fT-n}\right)^2\right] + \frac{1}{128}\sum_{n\epsilon S}\delta(fT-n). \quad (72)$$

Both the continuous and the discrete components are clearly discernible in this spectrum.

Figure 22 shows graphically the spectrum of this 8FSK scheme advocated by MITRE/Harris. Note the eight collocated density peaks and discrete lines at $fT=\pm1, \pm3, \pm5, \pm7$. The placement of peaks, if not their number, is consistent with other k=2 square-wave modulations (see Figure 4 for M=4 and Figure 16 for M=2). The nulls occur in the central region, that is for $|fT| \leq 8$, at even integers, while for $|fT| > 8$, nulls occur at every integer.

As implied, there are eight discrete spectral lines. They are separated by two fT units. Each spectral line has a power of 1/128. The definite integrals in Appendix B yield the fact that the continuous spectral component has a power content of 7/16. Therefore, the total discrete line power is 12.5 percent of the total 8FSK power.

Figure 23 confirms, on a log-log scale that for large fT the power density falls off as $(21/2\pi^2)(fT)^{-4}$.

11. CONCLUSIONS

There are three main conclusions to be drawn from this study:

First, the MFSK waveforms considered here represent only a few selected examples from an infinity of possible waveforms. The selection has been based on practical applications, as well as on mathematical tractability. For many other waveforms, one is hard pressed to express the power spectra with manageable formulas, as has been done here. More extensive computer runs then would seem to be the only way to produce the plots of power spectral density versus frequency. This can and should be done, whenever a particular waveform is proposed and its spectra need to be ascertained.

Second, all the pulse shapes considered here have discrete spectral lines. But one should not jump to the conclusion that it is so in general. The fact is (see the conditions given in Section 2) that for arbitrary symbol waveforms, with arbitrary symbol probabilities, one obtains line spectra whenever the modulation index k is an integer. If the index is not an integer, the line spectrum vanishes.

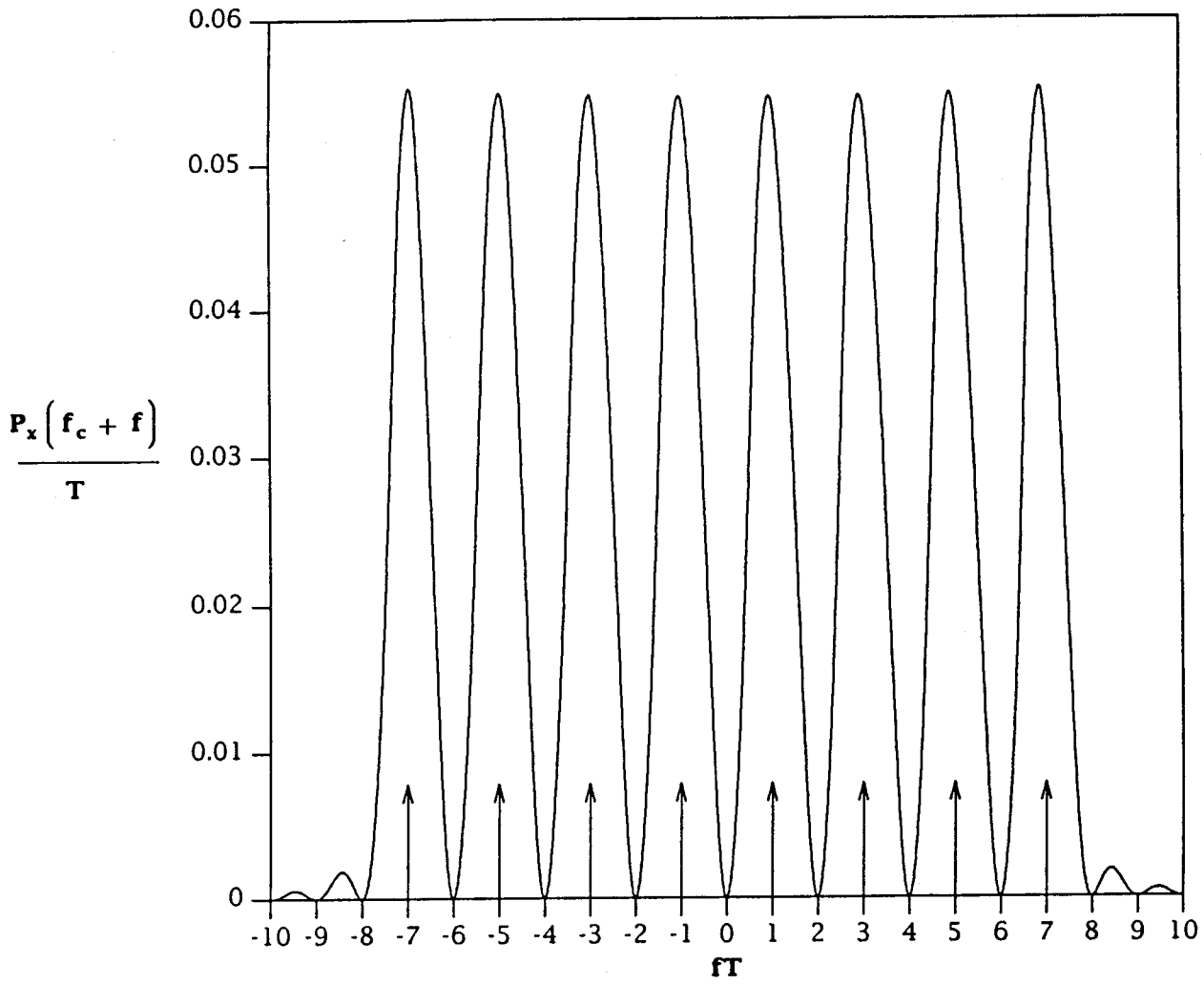

Figure 22. The continuous and discrete spectra of square-wave 8FSK for modulation index k = 2.

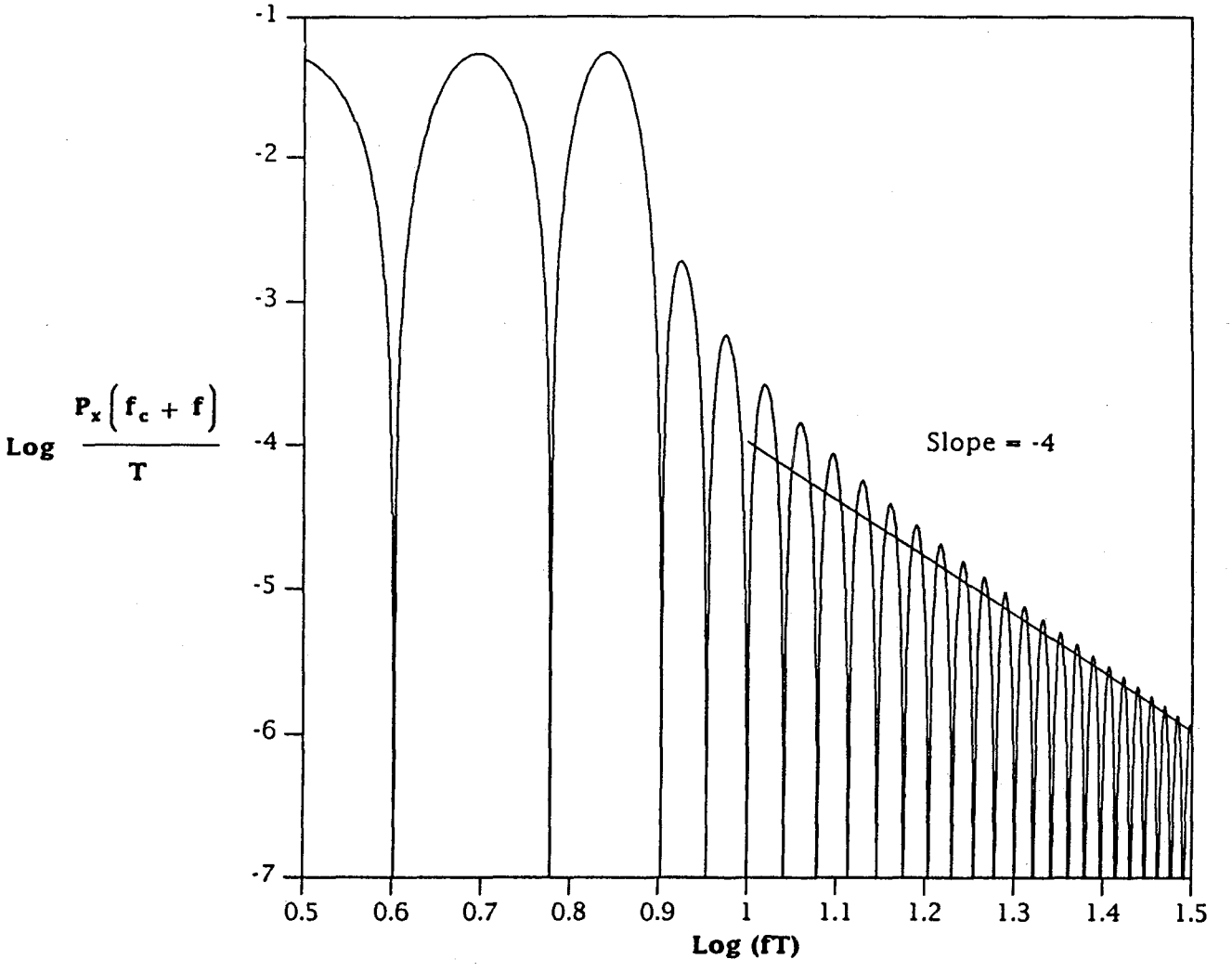

Figure 23. The asymptotic spectral behavior of the k = 2, square-wave, 8FSK for large frequencies.

Third, there is the issue of the asymptotic spectral slopes. For a raised-cosine pulse, the logarithm of the peak envelope of the continuous spectrum decays with a slope of -8 versus frequency f, as f tends to infinity. For a squared raised-cosine waveform, that slope is -12. For raised cosine to the n-th power, as no surprise, the asymptotic peak fall-off must be $-4(n+1)$, where $n=1,2,3 \ldots$. Because all such waveforms can be written as weighted sums of $\cos(2\pi\, mt/T)$, where $m=1,2,3 \ldots$, the spectral results involve infinite sums of finite products of ordinary Bessel functions. Thus, while arbitrarily steep slopes are possible, they do entail mathematical complexities that may not be worth the effort. Numerical methods remain as perhaps the only workable way to generate the corresponding spectra.

12. REFERENCES

Anderson, R.R., and J. Salz (1965), Spectra of digital FM, Bell Syst. Tech. J. 44, pp. 1165-1189.

Bennett, W.R., and S.O. Rice (1963), Spectral density and auto-correlation functions associated with binary frequency shift keying, Bell Syst. Tech. J. 42, pp. 2355-2385.

British Association for the Advancement of Science (1950), Bessel Functions, Part I; Math. Tables, Volume VI (Cambridge at the University Press, Cambridge, UK).

Gradshteyn, I.S., and I.M. Ryzhik (1980), Tables of Integrals, Series, and Products (Academic Press, New York, NY).

Lucky, R.W., J. Salz, and E.J. Weldon (1968), Principles of Data Communication (McGraw-Hill Book Co., New York, NY).

Papoulis, A. (1962), The Fourier Integral and Its Applications (McGraw-Hill Book Co., New York, NY).

Papoulis, A. (1965), Probability, Random Variables, and Stochastic Processes (McGraw-Hill Book Co., New York, NY).

Prabhu, V.K., and H.E. Rowe (1974), Spectra of digital phase modulation by matrix methods, Bell Syst. Tech. J. 53, pp. 899-935.

Rowe, H.E., and V.K. Prabhu (1975), Power spectrum of a digital, frequency-modulated signal, Bell Syst. Tech. J. 54, pp. 1095-1125.

Salz, J. (1965), Spectral density function of multilevel continuous-phase FM, IEEE Trans on Inform. Theory IT-11, pp. 429-433.

Taub, H., and D.L. Schilling (1971), Principles of Communication Systems (McGraw-Hill Book Co., New York, NY).

Watson, G.N. (1962), Theory of Bessel Functions (Cambridge at the University Press, Cambridge, UK).

APPENDIX A. SPECTRUM NOTATION USED BY SELECTED AUTHORS

To facilitate the comparison of MFSK power spectra derived by different workers, in particular the graphs and relevant equations, we present a brief digest of their notation. The list is selective with respect to authors and symbols.

Bennett and Rice (1963):

Spectral density $f_s W_u(f)/A^2$ is plotted versus $(f-f_1)/f_s$, where

A	Signal amplitude.
f_1	Lowest of the two binary-FSK frequencies.
f_s	Signaling or keying frequency or $1/T$.
$W_u(f)$	Spectral density function.

Anderson and Salz (1965):

Normalized spectral density $G(\beta)/A^2T$ is plotted versus β, where

A	Signal amplitude.
β	Normalized frequency or $(\omega-\omega_c)T/2\pi=(f-f_c)T$.
f_c	Carrier frequency.
$G(\beta)$	Spectral density.
T	Switching or keying interval.
ω_c	Angular carrier frequency or $2\pi f_c$.

Lucky, Salz, and Weldon (1968):

Normalized spectral density $V(\beta)/A^2T$ is plotted versus β, where

$V(\beta)$	Spectral density.
	[All other directly involved quantities are the same as in Anderson and Salz (1965)].

Prabhu and Rowe (1974), Rowe and Prabhu (1975):

Normalized spectral density $P_V(f)/T$ versus fT,

where

$P_V(f)$	Baseband spectral density.
T	Signaling or keying interval.
V	Same as $V(t)$; a complex angle modulated baseband signal with unity amplitude.

This report (1989):

Normalized spectral density $P_X(f_C + f)/T$ versus fT,

where

f_C	Carrier frequency.
$P_X(f_C + f)/T$	Spectral density of real signal x at frequency f from the carrier. [Same as $P_V(f)/2$ in Prabhu and Rowe (1974), also in Rowe and Prabhu (1975)].
T	Keying interval.
x	Same as $x(t)$; a real MFSK, unity amplitude signal at carrier frequency.

APPENDIX B. USEFUL TRIGONOMETRIC PROPERTIES

A number of trigonometric limits, definite integrals, and related identities are useful for spectral manipulation. This appendix collects in one place the most used properties. These properties, by all means, may be derived from the basics or found scattered through various texts. For what follows, our most used reference has been Gradshteyn and Ryzhik (1980).

Limit Values of Interest

$$\lim_{x \to n} \frac{\sin^2(\pi x)}{(x-n)^2} = \pi^2 \qquad \lim_{x \to n} \frac{\sin(2\pi x)}{x-n} = 2\pi$$

$$\lim_{x \to n+1/2} \frac{\cos^2(\pi x)}{(x-(n+1/2))^2} = \pi^2 \qquad \lim_{x \to n+1/2} \frac{\cos(2\pi x)}{x-(n+1/2)} = 2\pi$$

$$\lim_{x \to n} \frac{\sin^2(\pi x)}{x-n} = 0 \qquad \lim_{x \to n} \frac{1-e^{\pm j2\pi x}}{x-n} = \mp j2\pi$$

$$\lim_{x \to n+1/2} \frac{\cos^2(\pi x)}{x-(n+1/2)} = 0$$

Definite Integrals of Interest

For real α:

$$\int_0^\infty \frac{\sin(\alpha x)}{x}\, dx = \frac{\pi}{2} \operatorname{sgn} \alpha$$

$$\int_{-\infty}^{\infty} \frac{\sin^2(\alpha x)}{x^2}\, dx = \pi\alpha$$

For integer n:

$$\int_{-\infty}^{\infty} \frac{\sin^2(\pi x)}{(x \pm n)^2}\, dx = \int_{-\infty}^{\infty} \frac{\cos^2(\pi x)}{(x \pm (n+1/2))^2}\, dx = \pi^2$$

$$\int_{-\infty}^{\infty} \frac{\sin^2(\pi x)}{(x^2-n^2)^2}\, dx = \frac{\pi^2}{2n^2}$$

$$\int_{-\infty}^{\infty} \frac{\cos^2(\pi x)}{(x^2-(n+1/2)^2)^2}\,dx = \frac{\pi^2}{2(n+1/2)^2}$$

and for integers $n \neq m$:

$$\int_{-\infty}^{\infty} \frac{\sin^2(\pi x)}{(x^2-n^2)(x^2-m^2)}\,dx = \int_{-\infty}^{\infty} \frac{\cos^2(\pi x)}{(x^2-(n+1/2))^2(x^2-m+1/2)^2)}\,dx = 0$$

$$\int_{-\infty}^{\infty} \frac{x^2\sin^2(\pi x)}{(x^2-n^2)^2(x^2-m^2)^2}\,dx = \frac{\pi^2}{(n^2-m^2)^2}$$

$$\int_{-\infty}^{\infty} \frac{x^2\cos^2(\pi x)}{(x^2-(n+1/2)^2)^2(x^2-(m+1/2)^2)^2}\,dx = \frac{\pi^2}{(n-m)^2(n+m+1)^2}$$

APPENDIX C. USEFUL BESSEL FUNCTION PROPERTIES

Different Forms of the Generating Function

Start with the basic generating function for Bessel functions (Watson, 1962) in the form

$$e^{(z/2)(t-1/t)} = \sum_{n=-\infty}^{\infty} t^n J_n(z) \qquad \text{for } t \neq 0,$$

and note that a substitution $t=j\exp(j\theta)$ gives (35) in Section 4 of the main text. Another substitution, $t=\exp(j\theta)$, yields (43) in Section 5. The last version is used to get Fourier series coefficients $c_n]$ for the $q(t)]$ function in Section 6. Set $k=2$ in (51). Expand

$$e^{-j(4/3)\Delta]} \sin(2\pi t/T) = \sum_{n=-\infty}^{\infty} J_n(-(4/3)\Delta])e^{j2\pi nt/T},$$

$$e^{j(1/6)\Delta]} \sin(4\pi t/T) = \sum_{m=-\infty}^{\infty} J_m((1/6)\Delta])e^{j4\pi mt/T},$$

and substitute their product into (51). Then

$$q(t)] = \sum_{n,m=-\infty}^{\infty} J_{n-\Delta]-2m}(-(4/3)\Delta])J_m((1/6)\Delta])e^{j2\pi nt/T},$$

and by inspection

$$c_n] = \sum_{m=-\infty}^{\infty} J_{n-\Delta]-2m}(-(4/3)\Delta])J_m((1/6)\Delta])$$

$$= I_{n-\Delta]}(-(4/3)\Delta]),((1/6)\Delta]).$$

The last line is the quoted identity in Section 6, (52).

Properties of the Function $I_n(u,v)$

Function $I_n(u,v)$ is defined as the infinite sum of Bessel function products, see (53). To derive its integral identity, consider the standard integral definition of the Bessel function (Watson, 1962). This implies

$$I_m(u,v) = \frac{1}{(2\pi)^2} \sum_{m=-\infty}^{\infty} \int_{-\pi}^{\pi} e^{j(u\cos\phi+(n-2m)(\phi-\pi/2))}d\phi \cdot \int_{-\pi}^{\pi} e^{j(v\cos\theta+m(\theta-\pi/2))}d\theta$$

$$= \frac{1}{(2\pi)^2} \int_{-\pi}^{\pi} d\phi \int_{-\pi}^{\pi} d\theta e^{j(u\cos\phi+v\cos\theta+n(\phi-\pi/2))} \lim_{N\to\infty} \sum_{m=-N}^{N} e^{jm(\theta-2\phi+\pi/2)}.$$

This double integral can be reduced to a single integral with the help of the Fourier-series kernel (Papoulis, 1962), which asserts that

$$\lim_{N\to\infty} \sum_{m=-N}^{N} e^{j2\pi mt/T} = T \lim_{N\to\infty} \sum_{m=-N}^{N} \delta(t-mT).$$

Insertion of the kernel produces

$$I_n(u,v) = \frac{1}{2\pi} \int_{-\pi}^{\pi} e^{j(u\cos\theta+v\cos 2\theta+n(\theta-\pi/2))}d\theta$$

While simple in principle, this $I_n(u,v)$ integral tends to confuse the real and imaginary parts of the integrand. The fact that a change in variable, such as $\theta=\theta'+\pi/2$, generates

$$I_n(u,v) = \frac{1}{2\pi} \int_{-\pi}^{\pi} e^{-j(u\sin\theta+v\sin 2\theta-n\theta)}d\theta,$$

may appear at the first glance as not much of an improvement. However, when one discards the odd-symmetry parts around $\theta=0$, a completely real integral materializes:

$$I_n(u,v) = \frac{1}{\pi} \int_{0}^{\pi} \cos(u\sin\theta+v\sin 2\theta-n\theta)d\theta.$$

This is the formula cited for its apparent utility in (53) of Section 6. While it clearly can be modified and expressed in many other equivalent ways, none seem to possess enough advantages to displace the above.

Like the ordinary Bessel functions, whose generating function is (Watson, 1962)

$$\sum_{n=-\infty}^{\infty} t^n J_n(z) = e^{z/2(t-1/t)},$$

the $I_n(u,v)$ functions also possess a generating function:

$$\sum_{n=-\infty}^{\infty} t^n I_n(u,v) = e^{u/2(t-1/t) + v/2(t^2-1/t^2)}.$$

Generating functions are convenient to derive such identities as,

$$\begin{aligned}
\sum_{n=-\infty}^{\infty} n^j I_n(u,v) &= 1 && \text{if } j = 0,\\
&= u + 2v && = 1,\\
&= (u + 2v)^2 && = 2,\\
&= (u + 2v)^3 + (u + 8v) && = 3,\\
&= (u + 2v)^4 + 4(u + 2v)(u + 8v) && = 4,\\
&= (u + 2v)^5 + 10(u + 2v)^2(u + 8v) + (u + 32v) && = 5,
\end{aligned}$$

which are needed to ascertain asymptotic properties.

Neumann Series and Total Power in Discrete Spectral Lines

To prove the identity claimed in (40) for sine-wave pulses, use the Neumann Addition Theorem (Watson, 1962) in one of its simplest forms,

$$J_m(u-v) = \sum_{n=-\infty}^{\infty} J_{m+n}(u) J_n(v).$$

Then for m=0 and u=v=x,

$$1 = \sum_{n=-\infty}^{\infty} J_n^2(x),$$

while for m=0 and u=-v=x,

$$J_0(2x) = \sum_{n=-\infty}^{\infty} (-1)^n J_n^2(x).$$

Addition of the above yields

$$1 + J_0(2x) = 2 \sum_{n=-\infty}^{\infty} J_{2n}^2(x),$$

which for $x=k\pi/2$ and $x=3k\pi/2$ takes care of the two infinite sums of squares in (40). Likewise, setting u=3x, v=x, to be followed by u=3x, v=-x, and summing produces for m=0:

$$J_0(2x) + J_0(4x) = 2 \sum_{n=-\infty}^{\infty} J_{2n}(x) J_{2n}(3x).$$

For $x=k\pi/2$, this applies to the remaining cross-product term in (40).

To prove (49) for raised-cosine pulses, use the same Neumann Addition Theorem, but with different values of m. From (46) and (47), note that each B_n^2 contains four square terms and six cross-product terms. The square terms follow from m=0 and are all equal to unity. The cross-product terms are more complicated, but tractable, as shown next.

From m=2,

$$J_2(2) = \sum_{n=-\infty}^{\infty} J_{n-1}(1)\, J_{n+1}(-1) \qquad \text{if } u=-1,\ v=1,$$

$$= \sum_{n=-\infty}^{\infty} J_{n-1}(1)\, J_{n-3}(3) \qquad \text{if } u=1,\ v=3,$$

$$= \sum_{n=-\infty}^{\infty} J_{n+1}(-1)\ J_{n+3}(-3) \qquad \text{if } u=-3,\ v=-1.$$

From m=4,

$$J_4(4) = \sum_{n=-\infty}^{\infty} J_{n-1}(1)\ J_{n+3}(-3) \qquad \text{if } u=-3,\ v=1,$$

$$= \sum_{n=-\infty}^{\infty} J_{n+1}(-1)J_{n-3}(3) \qquad \text{if } u=-1,\ v=3.$$

Finally, from m=6,

$$J_6(6) = \sum_{n=-\infty}^{\infty} J_{n-3}(3)J_{n+3}(-3) \qquad \text{if } u=-3,\ v=3.$$

Substitution of these identities into (46) to (48) yields the right side of (49).

To evaluate the total power in the discrete spectra, it is sometimes expedient to use a generalization of Neumann's Addition Theorem in the form

$$I_m(u-s,\ v-t) = \sum_{n=-\infty}^{\infty} I_{m+n}(u,v)I_n(s,t).$$

It is proved by expanding its left side in the Bessel function series of (53).

A final result, useful to evaluate the $I_n(u,v)$ functions for fixed arguments u and v, is the recurrence relation:

$$u[I_{n-1}(u,v) + I_{n+1}(u,v)] + 2v[I_{n-2}(u,v) + I_{n+2}(u,v)] = 2nI_n(u,v).$$

Its proof follows from substituting the recurrence property of ordinary Bessel functions (Watson, 1962),

$$x[J_{n-1}(x) + J_{n+1}(x)] = 2nJ_n(x)$$

into the series definition of $I_n(u,v)$, as given in (53).

FORM **NTIA-29**
(4-80)

U.S. DEPARTMENT OF COMMERCE
NAT'L. TELECOMMUNICATIONS AND INFORMATION ADMINISTRATION

BIBLIOGRAPHIC DATA SHEET

	1. PUBLICATION NO.	2. Gov't Accession No.	3. Recipient's Accession No.
	NTIA Report 89-250		

4. TITLE AND SUBTITLE
Power Spectral Densities for Selected Digital Phase-Continuous MFSK Emissions

5. Publication Date
October 1989

6. Performing Organization Code
NTIA/ITS.N1

7. AUTHOR(S)
M. Nesenbergs, D. L. Smith, and L. T. Jones

9. Project/Task/Work Unit No.

8. PERFORMING ORGANIZATION NAME AND ADDRESS
National Telecommunications and Information Admin.
Institute for Telecommunication Sciences
325 Broadway
Boulder, CO 80303-3328

10. Contract/Grant No.

11. Sponsoring Organization Name and Address
National Telecommunications and Information Admin.
Herbert C. Hoover Building
14th and Constitution Avenue, NW
Washington, DC 20230

12. Type of Report and Period Covered

13.

14. SUPPLEMENTARY NOTES

15. ABSTRACT *(A 200-word or less factual summary of most significant information. If document includes a significant bibliography or literature survey, mention it here.)*

This report is a brief outline and a catalog of 11 power spectral densities for certain M-ary frequency shift keying waveforms. Spectral equations are displayed in graphical form for easy visualization. The spectra pertain to real signals centered on their carrier frequencies.

The selected waveforms are all phase-continuous with no symbol-to-symbol overlap. The number of keying waveforms, M, varies from 2 to 8. The modulation index, k, is typically 2, and only occasionally assumes values of 1 and 4. In all 11 cases considered one encounters discrete line spectra. The relative power contained in the discrete spectrum turns out to be 1/M for regular square waveforms with no dependence between successive symbols and somewhat larger for the other cases considered here. The asymptotic behavior of the continuous spectral component agrees with the theoretical predictions for very large frequency deviations.

Specific waveform shapes include square (or rectangular) pulses, sine-pulses, raised cosine pulses, and squared raised-cosine pulses. The concluding sections of the report cover two special systems of recent practical interest. They are the M=4 and k=2, alternating frequency, format of Rockwell/Collins and the M=8, k=2, scheme developed by MITRE and Harris Corporations.

Key words: asympotics; continuous and line spectra; M-ary frequency shift keying (MFSK); phase-continuous waveforms; spectral densities

17. AVAILABILITY STATEMENT	18. Security Class. *(This report)*	20. Number of pages
☒ UNLIMITED.	Unclassified	76
☐ FOR OFFICIAL DISTRIBUTION.	19. Security Class. *(This page)*	21. Price:
	Unclassified	

☆ U.S. GOVERNMENT PRINTING OFFICE: 1989—773-002/11007